
Unsteady Aerodynamic Load Estimates on Turning Vanes in the National Full-Scale Aerodynamic Complex

Thomas R. Norman

(NASA-TM-88191) UNSTEADY AERODYNAMIC LOAD
ESTIMATES ON TURNING VANES IN THE NATIONAL
FULL-SCALE AERODYNAMIC COMPLEX (NASA) 75 p
CSCL 01A

N87-15179

Unclas
G3/02 40343

December 1986



National Aeronautics and
Space Administration

Unsteady Aerodynamic Load Estimates on Turning Vanes in the National Full-Scale Aerodynamic Complex

Thomas R. Norman, Ames Research Center, Moffett Field, California

December 1986

NASA

National Aeronautics and
Space Administration

Ames Research Center
Moffett Field, California 94035

NOMENCLATURE

A_C	cross-sectional tunnel area, ft^2
\overline{AE}	air exchange ratio
A_R	area ratio $\frac{A_1}{A_2}$
A_T	vane truss area, ft^2
A_V	vane planform area, ft^2
a_1, a_2	"effective" lift or drag curve slope
C_{L_α}	two-dimensional lift curve slope
c	vane chord, ft
D	drag, lb
d	section drag, lb/ft
d_j	jet nozzle diameter, ft
$d_{1/2}$	distance from jet centerline to one-half velocity location, ft
H	total height of one vane, ft
h	vane section length, ft
L	lift, lb
l	section lift, lb/ft
N	number of vanes in vane set
P_s	static pressure, lb/ft^2
ΔP_T	total pressure loss, lb/ft^2
q	dynamic pressure, lb/ft^2
r_n	velocity ratio $(V/V_{0_{max}})$ across vane set
S	spectral function
$s(x)$	velocity ratio $(V/V_{0_{max}})$ along vane span

\overline{TI} turbulence intensity
 T_s static temperature, °F
 U_c jet velocity at jet centerline, ft/sec
 U_∞ free-stream velocity around jet, ft/sec
 u axial velocity, ft/sec
 V free-stream velocity, ft/sec
 V_0 time-averaged velocity of flow parallel to tunnel centerline, ft/sec
 w lateral velocity, ft/sec
 x_c distance from jet exit to end of jet core, ft
 Z total distance along stagger line, ft
 α angle of attack, deg
 β angle between free stream velocity vector and line perpendicular to stagger line, deg
 η_d viscous drag coefficient
 θ_1 stagger angle, deg
 ρ air density, slug/ft³
 σ root-mean-squared (rms) value
 Ω frequency, Hz
 Ω_b characteristic "break" frequency, Hz

Subscripts

m mean value
 u axial velocity
 w lateral velocity
 x axial direction
 y lateral direction

- 1 conditions upstream of vane set
- 2 conditions downstream of vane set

SUMMARY

Unsteady aerodynamic design loads have been estimated for each of the vane sets in the National Full-Scale Aerodynamic Complex (NFAC). These loads include estimates of local loads over one vane section and global loads over an entire vane set. The analytical methods and computer programs used to estimate these loads are discussed in this paper. In addition, the important computer input parameters are defined and the rationale used to estimate them is discussed. Finally, numerical values are presented for both the computer input parameters and the calculated design loads for each vane set.

INTRODUCTION

A major modification project was initiated at NASA Ames Research Center to expand the capabilities and improve the aerodynamic characteristics of the 40- by 80-Foot Wind Tunnel. Various aspects of this project have been reported in earlier papers, Corsiglia et al. (ref. 1). One modification is the installation of a new drive system, increasing the maximum attainable velocity in the 40- by 80-ft test section from 200 to 300 knots. Another modification is the construction of a new nonreturn wind tunnel leg with an 80- by 120-ft test section. This new tunnel leg, which shares the drive system with the 40 × 80 tunnel, is designed for a maximum test section velocity of 100 knots. A plan view of this entire 40 × 80/80 × 120 wind tunnel facility, called the National Full-Scale Aerodynamic Complex (NFAC), is shown in figure 1.

Also shown in figure 1 are the locations of eight sets of turning vane cascades (vane sets). These vane sets were built to turn air efficiently around corners and provide acceptable flow quality throughout the wind tunnel circuit. To ensure the structural integrity of the vane sets at the new design speeds of the modified facility, it became necessary to provide accurate estimates for the new, higher aerodynamic loads. These load estimates were required to include both local and global loads. The local loads, the forces on one vane section, could then be used to determine the structural strength requirements of the individual vanes. The global loads, the net forces on an entire vane set, could be used in the structural analysis of the vane set superstructure.

Analytical methods were developed to estimate the steady and unsteady components of the aerodynamic loads. Details of these methods are documented in references 2 and 3. These methods were then incorporated into separate computer programs to give numerical estimates for the loads. Reference 3 contains the estimates for

the steady loads. The estimates for the unsteady loads are presented in this report.

This report is divided into three sections. The first section discusses the analytical methods and the computer programs that were developed to estimate the unsteady loads. The second section defines the input parameters needed for the computer programs and discusses the rationale that was used to determine them. The final section presents numerical values for both the computer parameters and the final calculated design loads for each vane set.

ANALYTICAL METHODS

A general analytical method was developed to estimate the unsteady aerodynamic forces caused by flow-field turbulence on wind tunnel vane sets (ref. 2). This method calculates unsteady lift and drag, defined as the forces parallel and perpendicular to the vane set stagger line, by linearly perturbing the appropriate steady-state momentum equations and assuming that the forces are due only to free-stream turbulence. The effects of uncorrelated velocity fluctuations and unsteady aerodynamics are included in the method. The final derived results include three-dimensional analytical expressions for unsteady lift and drag. Computer programs were written to numerically integrate these expressions. For convenience, separate programs were written to estimate global and local loads.

This general method was used to estimate unsteady loads on vane sets 1, 2, 5, 6, and 8. For vane sets 3, 4, and 7, however, slightly different methods were required. Details of these methods can be found in appendices A and B. Separate computer programs were written for each method.

COMPUTER INPUT PARAMETERS

The computer programs required that a number of input parameters be specified. A list of these parameters is presented in table 1. In the following section, these parameters are defined and the rationale used in determining them for individual vane sets is discussed.

Vane Geometry

Many of the input parameters (Z , θ_1 , N , c , H , h , A_T , A_R) were determined from NFAC full-scale geometry measurements. Some of the most important of these measurements are presented in table 2. Reference 3 should be consulted for detailed geometry information.

Three of the input parameters, the stagger line length Z , the stagger angle θ_1 , and the number of lift carrying vanes N , are constants for each vane set in the NFAC. Figure 2 shows how Z and θ_1 are defined. The number of lift-carrying vanes N was assumed to equal the actual number of vanes for every vane set except vane set 6. For this vane set, the last four outside corner vanes (57 total) were assumed to carry no lift because the trailing-edge flaps on these vanes had been removed. This assumption provides for conservative load estimates since the same total load is carried by fewer vanes.

The individual vane chords c and vane heights H are constants for vane sets 1, 2, 6, and 8. The chord for vane set 5 is also a constant but the height of this vane set varies across the tunnel. For unsteady design load purposes, this height was assumed to equal the average vane set height across the tunnel (75.4 ft). Both the chord and the height are variables for vane sets 3, 4, and 7. These two input parameters were assumed to equal the values for typical vanes in the respective vane sets (see table 2). Information on the chords and heights for all eight vane sets can be found in reference 3.

The vane section lengths h are the lengths over which local loads are anticipated to be important. Two different section lengths were used for each vane set, with the total vane height always chosen as one of these lengths. The other length was chosen based on the individual vane sets' structural characteristics. In particular, for vane sets 1, 2, 5, 6, and 8, the length chosen was the distance between splitter plates. For vane set 7, the length was the distance between structural members. For vane sets 3 and 4, which have neither splitters nor structural members, the length was chosen to equal approximately one-half the total vane height.

The projected truss area A_T is defined as the area of the structural truss assembly attached to vane sets 3 and 4 that is perpendicular to the free-stream velocity. It was used to help estimate the drag forces on vane sets 3 and 4 (see appendix A). A_T was estimated to be 39.34 ft² for each vane of these vane sets (see ref. 3).

The area ratio A_R is defined as the vane set frontal area divided by the vane set frontal area minus any blockage. It was used in the load estimation procedure for vane set 7 (see appendix B). A_R was estimated to equal 1.35 for this vane set (see ref. 3).

Air Density

The air density ρ at each vane set was estimated using the ideal gas law, $\rho = P_S/RT_S$, where T_S and P_S are the static temperature and pressure and R is the gas constant for air ($R = 1715.64$ ft-lb/slugs-°R). T_S was assumed to be constant throughout both the 40 x 80 and the 80 x 120 wind tunnel circuits: $T_S = 70^\circ\text{F}$ (529.67°R) in the 40 x 80, $T_S = 60^\circ\text{F}$ (519.67°R) in the 80 x 120. P_S was estimated by scaling measured pressure data to the new design velocity (ref. 3). A list of the estimated static pressures and resultant densities for each vane set is presented in table 3.

Onset and Outflow Angles

The onset angle β_1 is defined as the angle between the stagger line normal and the free-stream inflow velocity V_1 . Similarly, the outflow angle β_2 is defined as the angle between the stagger line normal and the free-stream outflow velocity V_2 . The sign convention for these two angles is shown in figure 2.

Since experimental data were not available, it became necessary to assume values for the onset angles to estimate design loads. For vane sets 1, 5, and 6 of the 40 x 80, it was assumed that the onset angle could vary from the ideal tunnel centerline flow ($\beta_1 = \theta_1$) by approximately 3°. This angle variation corresponded to the angle between the wall and the tunnel centerline in the diffuser sections immediately preceding these vane sets.

For vane set 2, the onset angle was assumed to vary from the ideal centerline flow by $\pm 1^\circ$. This small variation was assumed because a long tunnel section of constant area precedes this vane set. The onset angle for vane set 8 was assumed to vary by $\pm 3^\circ$, even though this vane set also has a constant area section preceding it. This larger variation resulted from the uncertainty in the outflow angle of vane set 6.

For vane set 5 of the 80 x 120, the onset angle was allowed to vary from the ideal centerline flow by 0° to $+10^\circ$ for local loads estimates. These angle variations were deduced from full-scale stress measurements on a previous vane set 5 design. For global-loads estimates, the onset angle was assumed to equal that of the ideal centerline flow. This latter assumption was made because it was considered unlikely that substantial flow deviation would occur over the entire vane set. For vane set 7 of the 80 x 120, ideal centerline flow was assumed for estimating both local and global loads. This corresponds to $\beta_1 = \theta_1 = 0^\circ$.

The outflow angle β_2 was estimated for vane sets 1, 2, 5, 6, and 8 using data acquired in the 1/10-scale Vane Set Test Facility. These data showed that the average outflow angle was dependent on the onset angle. Figures showing this dependency can be found in reference 3. The 1/10-scale data were then corrected for full-scale Reynolds number effects by adding 1° of overturning to the measured data. To be conservative, this corrected outflow angle was then allowed to vary by $\pm 2^\circ$ for vane sets 1, 2, 5, and 8, and $\pm 3^\circ$ for vane set 6. An additional $\pm 3^\circ$ variation was allowed for vane set 5 when estimating local loads because of changes in the vane splay angle across the vane set.

The outflow angle for vane set 7 was estimated using data taken during testing of the 1/50-scale NFAC model (ref. 3).

Viscous Drag Coefficient

The viscous drag coefficient η_d is defined as the average total pressure loss for one vane pitch (the distance between vane centers) divided by the free-stream dynamic pressure. This coefficient was estimated for vane sets 1, 2, 5, 6, and 8 by

using data gathered during 1/10-scale testing. Like the outflow angle, it was determined that η_d was dependent on the onset angle β_1 . Figures showing this dependence can be found in reference 3. In addition, it was found that η_d varied from one vane pitch to another. Thus, to be conservative, η_d was chosen to equal the maximum loss coefficient measured in the 1/10-scale facility. An additional coefficient of 0.04 was then added to η_d to compensate for the increase in drag caused by grit or foreign particle buildup on the vanes from such things as jet exhaust.

For vane sets 3, 4, and 7, estimates of η_d were determined from pressure data taken during preliminary full-scale testing.

Velocity Ratio Profiles and Maximum Velocity

The velocity ratio profiles r_n and $s(x)$ are both defined as the local axial velocity divided by the peak axial velocity (V_{\max}) at a given vane set. In particular, r_n is the velocity ratio (V/V_{\max}) at different points across a vane set and $s(x)$ is the velocity ratio at different points along a vane height. The entire velocity field at a vane set can then be estimated by using these two profiles and the maximum velocity.

For the 40 x 80 vane sets 1, 2, 5, 6, and 8, the velocity ratio profiles were estimated by scaling dynamic pressure data measured in the 1/50-scale facility. The techniques used in this scaling process are detailed in appendix A of reference 3. The maximum velocities at these vane sets were then estimated by using another quantity provided by the scaling process. This quantity was an estimate of the maximum axial velocity divided by the average axial velocity (V_{\max}/V_{ave}). The maximum velocity at each vane set was then estimated by multiplying this factor by V_{ave} . V_{ave} was derived by conserving mass through the vane set (\overline{VS}) and the test section (\overline{TS}) such that

$$V_{\text{ave}} = \overline{AE} \frac{(\rho VA)_{\overline{TS}}}{(\rho A)_{\overline{VS}}} \quad (1)$$

where \overline{AE} is the air exchange ratio, ρ is the density, V is the axial velocity, and A is the cross-sectional tunnel area. For those vane sets (2, 3, 5, and 6) between the air exchange inlet and exit, \overline{AE} was assumed to equal 1.1 (a 10% increase in mass flow). For all other vane sets, \overline{AE} was assumed to equal 1.0. The test section and tunnel area information used to calculate V_{ave} is presented in tables 4 and 5, respectively.

Since experimental data were not available, the velocity ratio profiles for vane sets 4, 5, and 7 of the 80 x 120 were assumed to be constant across the tunnel, i.e., $V/V_{\max} = V/V_{\text{ave}} = 1.0$. Boundary layer effects were compensated for at vane sets 4 and 5 by reducing the tunnel dimensions by a displacement thickness of 0.5 ft on each wall (80 x 120 full-scale data, ref. 3). This then gives an "effective"

area of constant velocity which can be substituted into equation 1 to get V_{ave} . Displacement thicknesses were not included for vane set 7 as it was assumed that the upstream drive fans would cause sufficient mixing to energize the wall boundary layers.

Table 6 lists the maximum V/V_{ave} ratio, V_{ave} , and the subsequent V_{max} for each vane set.

Turbulence Intensity and Break Frequency

The lateral and axial turbulence intensities, TI_w and TI_u , are defined as the lateral and axial rms (root-mean-square) velocities divided by the steady local free-stream velocity. The break frequency Ω_b is defined as that frequency on the axial turbulent velocity power spectrum where the power is equal to one half of its value at zero frequency (its peak value).

TI_w , TI_u , and Ω_b were estimated at vane sets in the 40 x 80 by using the data taken in the NASA Langley 4- by 7-m wind tunnel. These Langley data consisted of hot-wire time histories taken at different tunnel speeds in front of vane sets A, B, and C (see fig. 3). From these data, axial and lateral turbulence intensities and break frequencies were determined. These Langley results are listed in table 7.

Turbulence intensities of the 40 x 80 were then assumed to equal the highest intensities from the Langley results at corresponding tunnel locations. Thus, turbulence intensities at the 40 x 80 vane sets 1, 2, and 6 were assumed equal to those at the Langley vane sets A, B, and C, respectively. In addition, the intensities at vane sets 3 and 5 were assumed to equal those of vane set B and the intensities at vane set 8 were assumed equal to those of vane set C.

Break frequency estimates in the 40 x 80 were determined with a Strouhal-type scaling of the Langley results. The scaling law used was $\Omega_b \propto (aV + b)/\ell$, where V is the velocity, ℓ is the characteristic length, and a and b are least-square coefficients. For this particular case, V was chosen to be the test section velocity and ℓ was chosen to be the square root of the cross-sectional area of the tunnel at the vane set. Substituting for ℓ and noting that $\Omega_{bLangley} = aV_{Langley} + b$, the equation for the break frequencies in the 40 x 80 becomes

$$\Omega_{b40 \times 80} = \frac{aV_{40 \times 80} + b}{A_{40 \times 80} / A_{Langley}} \quad (2)$$

The constants a and b were determined for vane sets 1, 2, 3, and 5, by performing the required least-squares analysis on the Langley data in table 7. (Only the three highest test section velocities were used to get a more conservative fit of the data.) The a and b constants were not required for vane sets 6 and 8, however, since the Langley data indicated that the break frequency was independent of

velocity at vane set C. The pertinent tunnel areas needed to complete the break frequency estimates are listed in table 5.

The turbulence intensities and break frequency for vane set 7 of the 80 x 120 were determined by using data from vane set C of the Langley tunnel. This determination involved the assumption that the turbulence quantities downstream of the fan drive were independent of the upstream tunnel configuration.

The turbulence intensities and break frequencies for vane sets 4 and 5 of the 80 x 120 were estimated using data taken in the 80 x 120 test section during preliminary full-scale testing in 1982. These data showed maximum axial and lateral turbulence intensities of 2.0% and 1.8%, respectively. In addition, the break frequency at a test section velocity of 142.7 ft/sec was determined to be approximately 3.5 Hz. The break frequencies at vane sets 4 and 5 were then determined by direct Strouhal scaling ($\Omega \propto V/l$) of the test section data, where V is the average velocity at the vane set of interest and l is the square root of the cross-sectional area at that location. The average velocities at the vane sets were estimated using equation (1).

Lift Curve Slope

The two-dimensional lift curve slope C_{L_α} was used to estimate the local loads on vane sets 3 and 4 (appendix A). For design load calculations, a lift curve slope of 2π was assumed (ideal flat plate).

Input Changes Due to Test Section Jet

A requirement existed to estimate the unsteady loads on those vane sets (1, 4, 5) immediately downstream of the wind tunnel test sections, assuming that two jet engines were operating there. To help accomplish this, a computer program was developed to estimate the velocity, turbulence intensity, and dynamic-pressure profiles as a function of distance behind the jets. Details of the method used in this program are presented in appendix B of reference 3. For estimating unsteady design loads, the turbulence intensities and densities were assumed constant across each vane set and equal to their centerline values.

Using this approach, the turbulence caused by a jet was estimated at vane set 1 of the 40 x 80 tunnel. It was found to be well below the free-stream turbulence intensity and therefore was not included in the unsteady load estimates for this vane set.

Unsteady loads on vane sets 4 and 5 of the 80 x 120 were determined assuming two 16,000-lb-thrust turbofan engines were operating in the test section at a free-stream tunnel speed of 100 knots. The important parameters describing these jet engines are listed in table 8. Also listed in this table are the computer-calculated densities, turbulence intensities, and velocities at vane sets 4 and 5.

The break frequency in the jet was estimated by Strouhal scaling of the break frequency of a 1-in.-diam unheated jet (ref. 4). The scaling law used was $\Omega_b \propto U_c/d_{1/2}$, where U_c is the centerline jet velocity at downstream location x and $d_{1/2}$ is the distance from the jet centerline to where the velocity is equal to one-half its centerline value. From reference 5, we find that

$$d_{1/2} = d_j \frac{x}{x_c} \quad x > x_c \quad (3)$$

where

$$x_c = d_j(4 + 12\mu)$$

$$\mu = U_\infty/U_c$$

d is the jet diameter, x_c is the distance from the jet to the end of the jet core, and U_∞ is the free-stream velocity outside the jet. Table 9 lists the information necessary to estimate the break frequencies at vane sets 4 and 5.

The velocity ratios needed for global load estimates for vane set 5 were determined by assuming that the two engines operating in the test section were separated by a distance of 42 ft (see ref. 3 for more details).

DESIGN LOAD ESTIMATES

Computer parameters representing each vane set were input into the appropriate computer programs to calculate design loads. These calculated loads included estimates of unsteady lift and drag in terms of power spectra and rms values. In addition, peak loads were estimated by multiplying the computer-calculated rms loads by a peak-to-rms ratio of 2.5. This ratio was determined to be typical of the peak-to-rms turbulence-intensity ratios in the Langley tunnel (see table 7) and it was assumed that it could be applied directly to the unsteady rms loads.

It should be noted that because of the manner of derivation (see ref. 2), the power spectral load estimates are of the two-sided variety. In other words, the spectral energy has been mathematically spread over both positive and negative frequencies. This can be mathematically stated as

$$\sigma = \int_{-\infty}^{+\infty} S \, d\Omega \quad (4)$$

where σ is the rms load, S is the one-dimensional power spectra, and Ω is the frequency.

The computer input parameters and results for each vane set are presented in the following listing:

Tunnel section	Vane set	Input parameters	Results	
		Tables	Figures	
40 x 80	1	10,11	4-8	
	2	12,13	9-13	
	3	14	14-17	
	5	15,16	18-21	
	6	17,18	22-26	
	8	19,20	27-31	
	80 x 120	4	21	32-37
		5	22,23	38-48
7		24	49-52	

A summary of the final rms and peak load estimates for each vane set is presented in tables 25 and 26.

These unsteady aerodynamic load estimates, along with the steady load estimates of reference 3, were significantly higher than the loads used during the original tunnel design. When these loads were included in a new structural analysis of the vane sets, it became obvious that design changes were required. The results of this analysis showed that each vane set in the NFAC needed modification, reinforcement, or replacement.

CONCLUDING REMARKS

Unsteady aerodynamic design loads have been estimated at each of the eight vane sets in the NFAC. These loads were estimated using computer programs based on analytical models. In this paper, the input parameters used in these programs have been defined and the rationale used in estimating them for particular vane sets has been discussed. In addition, the calculated design loads have been presented in terms of power spectra and rms and peak load values.

APPENDIX A

The unsteady loads on vane sets 3 and 4 were estimated using a procedure that modeled each vane as an isolated airfoil with an attached truss assembly. For this case, the true steady lift (the force perpendicular to the free-stream velocity V_1) is expressible as

$$L_T = q A_V C_{L_\alpha} \alpha \quad (A1)$$

where q is the dynamic pressure ($\rho V_1^2/2$), A_V is the planform area of the vane, C_{L_α} is the lift curve slope, and α is the angle of attack.

The true steady drag (the force parallel to V_1) is expressible as

$$D_T = q \eta_\ell \frac{A}{N} + q A_T \quad (A2)$$

where η_ℓ is the viscous drag (total pressure loss) coefficient, A is the cross-sectional tunnel area at the vane set, N is the number of vanes, and A_T is the frontal area of the truss assembly. The first term in equation (A2) represents the viscous forces on the vane and the second term represents the pressure forces on the truss assembly.

By dividing equations (A1) and (A2) by the total height of one vane, the true sectional lift and drag equations can be derived

$$\ell_T = qc C_{L_\alpha} \alpha \quad (A3)$$

$$d_T = q \eta_\ell \frac{Z \cos \theta_1}{N} + q \frac{A_T}{H} \quad (A4)$$

where c is the vane chord, Z is the distance along the stagger line, and H is the height of one vane. These true lift and drag quantities can then be resolved into forces perpendicular (ℓ) and parallel (d) to the vane, such that

$$\begin{aligned} \ell &= \ell_T \cos \alpha + d_T \sin \alpha \\ &= \frac{1}{2} \rho V_1^2 c C_{L_\alpha} \alpha \cos \alpha + \eta_\ell \frac{Z \cos \theta_1}{N} + \frac{A_T}{H} \sin \alpha \end{aligned} \quad (A5)$$

$$\begin{aligned} d &= d_T \cos \alpha - \ell_T \sin \alpha \\ &= \frac{1}{2} \rho V_1^2 \eta_\ell \frac{Z \cos \theta_1}{N} + \frac{A_T}{H} \cos \alpha - c C_{L_\alpha} \alpha \sin \alpha \end{aligned} \quad (A6)$$

Unsteady force equations can then be derived by linearly perturbing the latter two equations about the variables α and V_1 . This analysis yields the following equations

$$\delta l = \rho b_1 V_{1m} \delta V_1 + \frac{1}{2} \rho b_2 V_{1m}^2 \delta \alpha \quad (A7)$$

$$\delta d = \rho b_3 V_{1m} \delta V_1 + \frac{1}{2} \rho b_4 V_{1m}^2 \delta \alpha \quad (A8)$$

where the subscript m designates a mean (steady-state) value, and

$$\begin{aligned} b_1 &= cC_{L_\alpha} \alpha_m \cos \alpha_m + \eta_\ell \frac{Z \cos \theta_1}{N} + \frac{A_T}{H} \sin \alpha_m \\ b_2 &= cC_{L_\alpha} \cos \alpha_m - cC_{L_\alpha} \alpha_m \sin \alpha_m + \eta_\ell \frac{Z \cos \theta_1}{N} + \frac{A_T}{H} \cos \alpha_m \\ b_3 &= \eta_\ell \frac{Z \cos \theta_1}{N} + \frac{A_T}{H} \cos \alpha_m - cC_{L_\alpha} \alpha_m \sin \alpha_m \\ b_4 &= -\eta_\ell \frac{Z \cos \theta_1}{N} + \frac{A_T}{H} \sin \alpha_m - cC_{L_\alpha} \sin \alpha_m - cC_{L_\alpha} \alpha_m \cos \alpha_m \end{aligned}$$

From figure 2, it follows that α and V_1 can be defined as

$$\alpha = \tan^{-1} \frac{w}{u} \quad (A9)$$

$$V_1 = (u^2 + w^2)^{1/2} \quad (A10)$$

where u and w are the axial and lateral inflow velocities.

Perturbing these latter two equations yields

$$\delta \alpha = \frac{1}{1 + (w_m/u_m)^2} \left(\frac{\delta w}{u_m} - \frac{w_m}{u_m^2} \delta u \right) \quad (A11)$$

$$\delta V_1 = \frac{1}{2} (u_m^2 + w_m^2)^{1/2} (2u_m \delta u + 2w_m \delta w) \quad (A12)$$

For the purposes of this analysis, it has been assumed that the mean angle of attack of the vanes will be zero. This implies that $w_m = 0$ and $u_m = V_1 = V_0$ and yields

$$\delta\alpha = \frac{\delta w}{V_0} \quad (\text{A13})$$

$$\delta V_1 = \delta u \quad (\text{A14})$$

This angle-of-attack assumption does not affect the unsteady load estimates since the lift curve slope is nearly constant around this angle.

By substituting these last two equations into equations (A7) and (A8), the final perturbation equations become

$$\delta l = \frac{1}{2} \rho V_0 c a_1 \delta w \quad (\text{A15})$$

$$\delta d = \frac{1}{2} \rho V_0 c a_2 \delta u \quad (\text{A16})$$

where

$$a_1 = c C_{L_\alpha} + \eta_l \frac{Z \cos \theta_1}{cN} + \frac{A_T}{cH}$$

$$a_2 = 2\eta_l \frac{Z \cos \theta_1}{cN} + 2 \frac{A_T}{cH}$$

These final equations were then incorporated into the procedures of reference 2 to provide estimates of the unsteady aerodynamics forces on vane sets 3 and 4. Note that the lift and drag estimates from this method are perpendicular and parallel to the vanes, not to the stagger line as with the other vane sets.

APPENDIX B

The unsteady loads on vane set 7 were estimated using a procedure that accounts for accelerating flow through a vane set caused by structural blockage, screens, etc. This was done by rederiving the momentum equations to incorporate this effect.

Using the variables as presented in figure 53, the lift on a vane set can be determined to be

$$L = V_{y_1} \rho V_{x_1} A_1 - V_{y_2} \rho V_{x_2} A_2 \quad (B1)$$

where A_1 is the vane set frontal area and A_2 is the frontal area minus any blockage. Incorporating the conservation of mass equation

$$\rho V_{x_1} A_1 = \rho V_{x_2} A_2 \quad (B2)$$

results in

$$L = \rho V_{x_1} A_1 (V_{y_1} - V_{y_2}) \quad (B3)$$

Similarly, it can be shown the drag on a vane set is

$$D = \rho V_{x_1} A_1 (V_{x_1} - V_{x_2}) + A_1 (P_1 - P_2) \quad (B4)$$

Bernoulli's equation is used to find an expression for $(P_1 - P_2)$ such that

$$P_1 - P_2 = \frac{1}{2} \rho (V_2^2 - V_1^2) + \Delta P_T \quad (B5)$$

Conservation of mass implies

$$V_{x_2} = V_{x_1} \frac{A_1}{A_2} = V_{x_1} A_R \quad (B6)$$

In addition, it can be shown that

$$V_{x_1} = V_1 \cos \beta_1 \quad (B7)$$

$$V_{y_1} = V_1 \sin \beta_1 \quad (B8)$$

$$V_{x_2} = V_2 \cos \beta_2 \quad (B9)$$

$$V_{y_2} = V_2 \sin \beta_2 \quad (B10)$$

Substituting these latter six equations into equations (B3) and (B4) yields

$$L = \rho A_1 V_1^2 \cos^2 \beta_1 (\tan^2 \beta_1 - A_R \tan^2 \beta_2) \quad (B11)$$

$$D = \frac{1}{2} \rho A_1 V_1^2 \left(2(1 - A_R) \cos^2 \beta_1 + A_R^2 \frac{\cos^2 \beta_1}{\cos^2 \beta_2} + \eta_\ell - 1 \right) \quad (B12)$$

where η_ℓ is the viscous loss coefficient equal to $\Delta P_T / [(1/2)\rho V_1^2]$.

By dividing these latter two equations by the total span of the vanes, the sectional lift and drag equations can be derived

$$\ell = \rho V_1^2 \frac{Z}{N} \cos^2 \beta_1 (\tan \beta_1 - A_R \tan \beta_2) \quad (B13)$$

$$d = \frac{1}{2} \rho V_1^2 \frac{Z}{N} \left(2(1 - A_R) \cos^2 \beta_1 + A_R^2 \frac{\cos^2 \beta_1}{\cos^2 \beta_2} + \eta_\ell - 1 \right) \quad (B14)$$

where Z is the total distance along the vane set stagger line and N is the number of vanes.

Unsteady force equations can then be derived by linearly perturbing these latter two equations about the variables V_1 and β_1 , with β_2 assumed constant. This analysis yields the following equations

$$\delta \ell = b_1 V_{1m} \delta V_1 + b_2 V_{1m}^2 \delta \beta_1 \quad (B15)$$

$$\delta d = b_3 V_{1m} \delta V_1 + b_4 V_{1m}^2 \delta \beta_1 \quad (B16)$$

where the subscript m designates a mean (steady-state) value, and

$$b_1 = 2\rho \frac{Z}{N} \cos^2 \beta_{1m} \left(\tan \beta_{1m} - A_R \tan \beta_2 \right)$$

$$b_2 = \rho \frac{Z}{N} \left(\cos^2 \beta_{1m} - \sin^2 \beta_{1m} + 2A_R \cos \beta_{1m} \sin \beta_{1m} \tan \beta_2 \right)$$

$$b_3 = \rho \frac{Z}{N} \left[\left(2(1 - A_R) + \frac{A_R^2}{\cos^2 \beta_2} \right) \cos^2 \beta_{1m} + \eta_\ell - 1 \right]$$

$$b_4 = \rho \frac{Z}{N} \left[\left(-2(1 - A_R) + \frac{A_R^2}{\cos^2 \beta_2} \right) \cos \beta_{1m} \sin \beta_{1m} \right]$$

These final equations are in the exact form required for estimating unsteady loads using the method outlined in reference 2.

REFERENCES

1. Corsiglia, V. R.; Olson, L. E.; and Falarski, M. D.: Aerodynamic Characteristics of the 40- by 80/80- by 120-Foot Wind Tunnel at NASA Ames Research Center. NASA TM 85946, 1984.
2. Norman, T. R.; and Johnson, W.: Estimating Unsteady Aerodynamic Forces on a Cascade in a Three Dimensional Turbulence Field. NASA TM 86701, 1985.
3. Aoyagi, K.; and Olson, L. E.: Time Averaged Aerodynamic Loads of the 40- by 80-/80- by 120-Foot Wind Tunnel Vane Sets at NASA Ames Research Center. NASA TM 89413, to be published.
4. Corrsin, S.; and Uberoi, M. S.: Spectrums and Diffusion in a Round Turbulent Jet. NACA TN 2124, 1950.
5. Hinze, J. O.: Turbulence. McGraw-Hill, Inc., 1975, pp. 534-558.

TABLE 1.- COMPUTER INPUT PARAMETERS

Description	Symbol	Use ^a
Vane chord	c	5
Height of one vane	H	1,3
Vane section length over which local loads are estimated	h	2,3
Distance along stagger line	Z	5
Number of vanes in vane set	N	5
Viscous drag coefficient	η_d	5
Frontal area of supporting truss assembly	A_T	3
Free-stream onset angle	β_1	1,2
Free-stream outflow angle	β_2	1,2
Stagger angle	θ_1	5
Maximum free-stream velocity	$V_{0_{max}}$	5
Air density	ρ	5
Break frequency	ω_b	5
Lateral turbulence intensity	TI_w	5
Axial turbulence intensity	TI_u	5
Two-dimensional lift curve slope	C_{L_α}	3
Velocity ratio ($V/V_{0_{max}}$) along a vane height	$s(x)$	1
Velocity ratio ($V/V_{0_{max}}$) at each vane	r_n	1
Area ratio (Vane set area)/(Area - blockage)	A_R	4

- ^a1, global-load estimates for vane sets 1, 2, 5, 6, 7, and 8.
 2, local-load estimates for vane sets 1, 2, 5, 6, 7, and 8.
 3, vane sets 3 and 4 estimates.
 4, vane set 7 estimates only.
 5, all load estimates.

TABLE 2.- VANE SET GEOMETRY

Parameter	Vane set							
	1	2	3 (Vane 3H)	4 (Vane 4C)	5	6	7	8
Chord, ft	6.0	6.0	21.7	33.91	6.67	17.2	10.54	3.0
Vane height, ft	68.6	68.6	68.3	69.3	75.4 (average)	132.5	197.2	132.5
Distance between splitter plates or structural members, ft	11.4	11.4	68.3	69.3	25.1	1.0	17.8	11.0
Stagger line distance, ft	153.75	153.75	153.8	169.7	128.5	244.0	128.7	244.0
Stagger angle, °	45	45	45	45	-25.6 (40x80) 19.4 (80x120)	45	0	45
Number of vanes	50	50	7	5	36	57	12	159

TABLE 3.- STATIC PRESSURES AND DENSITIES

Vane set	Static pressure, lbf/ft ²	Density, slug/ft ³
1	2066.6	0.002274
2	2066.6	.002274
3	2065.8	.002273
4	2072.0	.002321
5 (40×80 mode)	2061.8	.002269
5 (80×120 mode)	2064.3	.002313
6	2134.8	.002349
7	2128.2	.002385
8	2134.8	0.002349

TABLE 4.- TEST SECTION CONDITIONS

40x80	
Static temperature T_s	70°F
Static pressure P_s	1861.8 lbf/ft ²
Density.....	0.002047 slug/ft ³
Area with acoustic liner.....	2754.59 ft ²
Velocity.....	506.4 ft/sec (300 knots)
80x120	
Static temperature.....	60°F
Static pressure.....	2078.8 lb/ft ²
Density.....	0.002329 slug/ft ³
Area.....	9600 ft ²
Displacement thickness on each wall.....	0.5 ft
Effective area.....	9401 ft ²
Velocity.....	168.8 ft/sec (100 knots)

TABLE 5.- TUNNEL AREAS AT
VANE SETS

Vane set	Area, ft ²
40x80	
1	7455.8
2	7455.8
3	7810.7
5	8737.8
6	22856.0
8	22856.0
80x120	
4	8568.0 (actual) 8378.0 (effective)
5	9138.5 (actual) 8943.0 (effective)
7	25380.0 (actual)
Langley 4x7	
A	850.5
B	929.3
C	2835.8

TABLE 6.- VELOCITY DATA

Vane set	Maximum velocity ratio, $(V/V_{ave})_{max}$	Average velocity V_{ave} , ft/sec	Maximum velocity $V_{0_{max}}$, ft/sec
1	1.48	168.4	248.5
2	1.22	185.2	225.8
3	1.22	185.2	225.8
4	1.0	190.1	190.1
5 (40x80 mode)	1.36	158.4	214.9
5 (80x120 mode)	1.0	178.7	178.7
6	1.42	58.5	83.1
7	1.0	62.78	62.78
8	1.24	53.2	65.9

TABLE 7.- TURBULENCE DATA AT LANGLEY 4x7-m WIND TUNNEL

Vane set	Test section velocity, ft/sec	Break frequency, Hz	Turbulence intensity		Peak-to-rms turbulence-intensity ratio
			Axial	Lateral	
A	58.0	2.8	0.071	0.101	2.7
	166.3	5.2	.092	.128	2.8
	223.1	6.0	.104	.144	2.8
	295.8	6.8	.115	.156	2.4
B	60.1	3.0	.048	.062	2.5
	150.5	3.0	.073	.092	2.6
	222.8	4.0	.084	.096	2.6
	295.5	4.6	.098	.111	1.8
C	62.0	3.4	.058	.080	2.4
	150.0	3.8	.076	.108	2.3
	223.1	4.0	.080	.114	2.1
	295.0	4.0	.104	.149	2.5

TABLE 8.- 80x120 TEST SECTION JET ENGINE PARAMETERS

Turbofan		
Diameter of jet, ft.....	2.0	
Velocity of jet at core, ft/sec.....	2046	
Static temperature of jet core, °F.....	616	
Density of air in jet core, slug/ft ³00122	
Mach number in jet core.....	1.27	
Free-stream conditions at jet location		
Velocity of free stream, ft/sec.....	168.9	
Static temperature of free stream, °F.....	60	
Static pressure of free stream, lbf/ft ³	2113.2	
Results	Vane set 4	Vane set 5
Distance downstream of jet, ft	205	303
Centerline velocity, ft/sec	249.3	234.7
Centerline turbulence intensity	.090	.068
Centerline density, slug/ft ³	.002241	.002313

TABLE 9.- BREAK FREQUENCY CAUSED BY JET

Parameter	Symbol	Reference jet (see ref. 5)	Jet at vane set 4	Jet at vane set 5
Jet diameter, ft	d	0.0833	2.0	2.0
Downstream distance behind jet, ft	x	1.6667	205.0	303.0
Centerline velocity at location x, ft/sec	U_{CL}	38.6	249.3	234.7
Free-stream velocity at jet, ft/sec	U_{∞}	0	168.9	168.9
Jet core velocity, ft/sec	U_c	---	2046	2046
Break frequency, Hz	Ω_b	57.3	3.85	2.45

TABLE 10.- 40x80 DESIGN LOAD PARAMETERS--
VANE SET 1

Parameter	Local lift	Local drag	Global lift
	Local drag		Global drag
c	6.0	6.0	6.0
H	---	---	68.6
h	11.4	68.6	---
Z	153.75	153.75	153.75
N	50	50	50
η_d	.114	.114	.114
β_1	42	42	42
β_2	-49	-49	-49
θ_1	45	45	45
$V_{0\max}$	248.5	248.5	248.5
ρ	.002274	.002274	.002274
Ω_b	3.0	3.0	3.0
TI_w	.156	.156	.156
TI_u	.115	.115	.115
$s(x)$	---	---	See table 11
r_n	---	---	See table 11

TABLE 11.- VANE SET 1 VELOCITY PROFILES

Vane no.	Velocity ratio r_n	Vane no.	Velocity ratio r_n	Vane no.	Velocity ratio r_n
1	0.579	18	0.986	35	0.997
2	.650	19	.971	36	1.000
3	.721	20	.947	37	.999
4	.792	21	.906	38	.997
5	.862	22	.857	39	.994
6	.922	23	.809	40	.992
7	.953	24	.760	41	.987
8	.980	25	.700	42	.976
9	.988	26	.653	43	.965
10	.995	27	.697	44	.936
11	.995	28	.756	45	.902
12	.995	29	.798	46	.863
13	.995	30	.840	47	.793
14	.995	31	.883	48	.712
15	.995	32	.925	49	.623
16	.995	33	.968	50	.502
17	.993	34	.991		

Normalized vertical distance, x/H	Velocity ratio $s(x)$
0.000	0.000
.013	.378
.125	.675
.225	.885
.316	.971
.325	.994
.471	1.000
.604	1.000
.694	.97
.788	.861
.863	.715
.944	.607
.991	.484
1.000	0.000

TABLE 12.- 40x80 DESIGN LOAD PARAMETERS--
VANE SET 2

Parameter	Local lift Local drag	Local drag	Global lift Global drag
c	6.0	6.0	6.0
H	---	---	68.6
h	11.4	68.6	---
Z	153.75	153.75	153.75
N	50	50	50
η_d	.116	.116	.116
β_1	46	46	46
β_2	-47	-47	-47
θ_1	45	45	45
$V_{0\max}$	225.8	225.8	225.8
ρ	.002273	.002273	.002273
Ω_b	2.4	2.4	2.4
TI_w	.111	.111	.111
TI_u	.098	.098	.098
s(x)	---	---	See table 13
r_n	---	---	See table 13

TABLE 13.- VANE SET 2, VELOCITY PROFILES

Vane no.	Velocity ratio r_n	Vane no.	Velocity ratio r_n	Vane no.	Velocity ratio r_n
1	0.710	18	0.989	35	0.961
2	.772	19	.983	36	.972
3	.785	20	.963	37	.979
4	.749	21	.943	38	.988
5	.684	22	.914	39	.982
6	.686	23	.880	40	.982
7	.774	24	.845	41	.970
8	.868	25	.826	42	.959
9	.902	26	.812	43	.948
10	.936	27	.809	44	.937
11	.955	28	.809	45	.926
12	.970	29	.826	46	.915
13	.985	30	.648	47	.903
14	.999	31	.871	48	.882
15	.999	32	.893	49	.808
16	1.000	33	.916	50	.734
17	.994	34	.939	51	0.000

Normalized vertical distance, x/H	Velocity ratio $s(x)$
0.000	0.000
.015	.588
.075	.782
.113	.818
.204	.885
.263	.941
.313	.966
.375	.996
.438	1.000
.500	.989
.550	.981
.619	.947
.688	.917
.731	.885
.781	.842
.838	.804
.888	.766
.963	.746
.988	.663
1.000	0.000

TABLE 14.- 40x80 DESIGN LOAD
INPUTS--VANE SET 3

Parameters	Local lift Local drag	Local lift Local drag
c	21.7	21.7
H	68.3	68.3
h	34	68.3
Z	153.8	153.8
N	7	7
η_d	.105	.105
A_T	39.34	39.34
θ_1	45	45
$V_{0\max}$	225.8	225.8
ρ	.002273	.002273
Ω_b	2.4	2.4
TI_w	.111	.111
TI_u	.098	.098
$C_{L\alpha}$	6.28	6.28

TABLE 15.- 40x80 DESIGN LOAD PARAMETERS--
VANE SET 5

Parameters	Local lift	Local drag	Global lift	Global drag
c	6.67	6.67	6.67	6.67
H	---	---	75.4	75.4
h	25.1	75.4	---	---
Z	128.5	128.5	128.5	128.5
N	36	36	36	36
η_d	.105	.120	.105	.120
β_1	-22.6	-28.6	-28.6	-22.6
β_2	-31.3	-32.1	-29.1	-28.3
θ_1	-25.6	-25.6	-25.6	-25.6
$V_{0\max}$	214.9	214.9	214.9	214.9
ρ	.002269	.002269	.002269	.002269
Ω_b	2.2	2.2	2.2	2.2
TI_w	.111	.111	.111	.111
TI_u	.098	.098	.098	.098
$s(x)$	---	---	See table 16	See table 16
r_n	---	---	See table 16	See table 16

TABLE 16.- VANE SET 5 (40x80),
VELOCITY PROFILES

Vane no.	Velocity ratio r_n	Vane no.	Velocity ratio r_n
1	0.695	19	0.833
2	.726	20	.831
3	.741	21	.846
4	.753	22	.868
5	.798	23	.890
6	.870	24	.912
7	.933	25	.934
8	.969	26	.957
9	.979	27	.973
10	.987	28	.977
11	.996	29	.969
12	.998	30	.963
13	.991	31	.963
14	.967	32	.929
15	.944	33	.916
16	.920	34	.902
17	.881	35	.889
18	.860	36	.826

Normalized vertical distance, x/H	Velocity ratio $s(x)$
0.000	0.000
.006	.526
.021	.618
.129	.838
.306	.999
.376	1.000
.447	.985
.506	.984
.527	.976
.600	.987
.741	.921
.800	.871
.839	.843
.939	.704
.965	.704
.976	.674
.988	.561
1.000	0.000

TABLE 17.- 40x80 DESIGN LOAD PARAMETERS--VANE SET 6

Parameters	Local lift	Local drag	Local drag	Global lift	Global drag
c	17.2	17.2	17.2	17.2	17.2
H	---	---	---	132.5	132.5
h	11	11	132.5	---	---
Z	244.0	244.0	244.0	244.0	244.0
N	53	53	53	53	53
η_l	.82	.97	.97	.82	.97
β_1	48.4	41.6	41.6	48.4	41.6
β_2	-48.0	-48.0	-48.0	-48.0	-48.0
θ_1	45	45	45	45	45
V_0	83.1	83.1	83.1	83.1	83.1
ρ_{max}	.002349	.002349	.002349	.002349	.002349
Ω_b	1.5	1.5	1.5	1.5	1.5
TI_w	.149	.149	.149	.149	.149
TI_u	.104	.104	.104	.104	.104
s(x)	---	---	---	See table 18	See table 18
r_n	---	---	---	See table 18	See table 18

TABLE 18.- VANE SET 6 VELOCITY PROFILES

Vane no.	Velocity ratio r_n	Vane no.	Velocity ratio r_n	Vane no.	Velocity ratio r_n
1	0.919	19	0.782	37	0.855
2	.919	20	.778	38	.849
3	.919	21	.774	39	.843
4	.875	22	.770	40	.837
5	.853	23	.766	41	.820
6	.847	24	.762	42	.800
7	.840	25	.774	43	.797
8	.837	26	.796	44	.815
9	.845	27	.818	45	.834
10	.853	28	.840	46	.852
11	.849	29	.848	47	.871
12	.837	30	.810	48	.889
13	.822	31	.837	49	.920
14	.801	32	.866	50	.961
15	.781	33	.879	51	.970
16	.761	34	.873	52	.975
17	.741	35	.867	53	.979
18	.720	36	.861	54	0.000

Normalized vertical distance, x/H	Velocity ratio $s(x)$
0.000	0.000
.005	.816
.019	.921
.051	.900
.070	.878
.108	.878
.146	.878
.191	.926
.242	.976
.318	.886
.382	.816
.425	.756
.477	.802
.510	.816
.573	.923
.605	.964
.656	1.000
.732	.956
.777	.939
.828	.939
.892	.939
.968	.939
.994	.811
1.000	0.000

TABLE 19.- 40x80 DESIGN LOAD PARAMETERS--VANE SET 8

Parameters	Local lift	Local drag	Local drag	Global lift	Global drag
c	3.0	3.0	3.0	3.0	3.0
H	---	---	---	132.5	132.5
h	11.0	11.0	132.5	---	---
Z	244	244	244	244	244
N	159	159	159	159	159
η_l	.164	.216	.216	.164	.216
β_1	48	42	42	48	42
β_2	-49.8	-51.8	-51.8	-49.8	-51.8
θ_1	45	45	45	45	45
V_{0max}	65.9	65.9	65.9	65.9	65.9
ρ	.002349	.002349	.002349	.002349	.002349
Ω_b	1.5	1.5	1.5	1.5	1.5
TI_w	.149	.149	.149	.149	.149
TI_u	.104	.104	.104	.104	.104
s(x)	---	---	---	See table 20	See table 20
r_n	---	---	---	See table 20	See table 20

TABLE 20.- VANE SET 8 VELOCITY PROFILES

Vane no.	Velocity ratio r_n	Vane no.	Velocity ratio r_n	Vane no.	Velocity ratio r_n
1	0.912	47	0.916	93	0.979
2	.993	48	.918	94	.976
3	.984	49	.919	95	.973
4	.975	50	.920	96	.970
5	.966	51	.922	97	.968
6	.957	52	.923	98	.965
7	.949	53	.924	99	.963
8	.940	54	.926	100	.960
9	.935	55	.927	101	.958
10	.935	56	.928	102	.956
11	.935	57	.930	103	.953
12	.935	58	.931	104	.951
13	.935	59	.933	105	.948
14	.935	60	.936	106	.946
15	.935	61	.940	107	.943
16	.935	62	.943	108	.941
17	.935	63	.946	109	.938
18	.938	64	.949	110	.936
19	.942	65	.953	111	.930
20	.946	66	.956	112	.922
21	.950	67	.959	113	.914
22	.953	68	.962	114	.907
23	.957	69	.966	115	.899
24	.961	70	.968	116	.891
25	.957	71	.969	117	.884
26	.952	72	.970	118	.876
27	.947	73	.971	119	.868
28	.942	74	.971	120	.861
29	.937	75	.972	121	.853
30	.932	76	.973	122	.845
31	.927	77	.974	123	.838
32	.922	78	.974	124	.830
33	.917	79	.977	125	.822
34	.912	80	.981	126	.815
35	.906	81	.984	127	.807
36	.901	82	.988	128	.799
37	.903	83	.991	129	.791
38	.904	84	.995	130	.781
39	.905	85	.998	131	.770
40	.907	86	.998	132	.759
41	.908	87	.996	133	.748
42	.909	88	.993	134	.737
43	.911	89	.990	135	.726
44	.912	90	.987	136	.716
45	.914	91	.984	137	.795
46	.915	92	.982	138	.694

TABLE 20.- CONCLUDED

Vane no.	Velocity ratio r_n	Vane no.	Velocity ratio r_n	Vane no.	Velocity ratio r_n
139	0.683	146	0.658	153	0.591
140	.672	147	.648	154	.581
141	.661	148	.639	155	.572
142	.661	149	.629	156	.562
143	.661	150	.620	157	.553
144	.661	151	.610	158	.543
145	.661	152	.600	159	.534

Normalized vertical distance, x/H	Velocity ratio $s(x)$
0.000	0.000
.005	.632
.059	.848
.141	.884
.168	.884
.303	.984
.859	1.000
.680	.945
.713	.919
.797	.942
.965	.848
.995	.729
1.000	0.000

TABLE 21.- 80x120 DESIGN LOAD PARAMETERS--VANE SET 4

Parameters	Local lift (without jet)	Local lift (without jet)	Local lift Local drag (with jet)	Local lift Local drag (with jet)
c	33.91	33.91	33.91	33.91
H	69.3	69.3	69.3	69.3
h	34	69.3	34	69.3
Z	169.7	169.7	169.7	169.7
N	5	5	5	5
n_d	.129	.129	.129	.129
A_T	39.34	39.34	39.34	39.34
θ_1	45	45	45	45
$V_{O_{max}}$	190.1	190.1	249.3	249.3
ρ	.002321	.002321	.002241	.002241
Ω_b	4.8	4.8	3.85	3.85
TI_w	.02	.02	.09	.09
TI_u	.018	.018	.09	.09
C_{L_α}	6.28	6.28	6.28	6.28

TABLE 22.- 80x120 DESIGN LOAD PARAMETERS--VANE SET 5

Parameters	Local lift (without jet)	Local lift Local drag (without jet)	Global lift Global drag (without jet)	Local lift (with jet)	Local lift Local drag (with jet)	Global lift Global drag (with jet)
c	6.67	6.67	6.67	6.67	6.67	6.67
H	---	---	75.4	---	---	75.4
h	25.1	75.4	---	25.1	75.4	---
Z	128.5	128.5	128.5	128.5	128.5	128.5
N	36	36	36	36	36	36
η_d	.313	.313	.313	.313	.313	.313
β_1	29.4	29.4	19.4	29.4	29.4	19.4
β_2	-31.05	-31.05	-28.05	-31.05	-31.05	-28.05
θ_1	19.4	19.4	19.4	19.4	19.4	19.4
$V_{O_{max}}$	178.7	178.7	178.7	234.7	234.7	234.7
ρ	.002313	.002313	.002313	.002313	.002313	.002313
Ω_b	4.5	4.5	4.5	2.45	2.45	2.45
TI_w	.02	.02	.02	.068	.068	.068
TI_u	.018	.018	.018	.068	.068	.068
$s(x)$	---	---	Flat profile	---	---	Table 23
r_n	---	---	Flat profile	---	---	Table 23

TABLE 23.- VANE SET 5, VELOCITY
PROFILE (80x120), TEST
SECTION JET

Vane no.	Velocity ratio r_n	Vane no.	Velocity ratio r_n
1	0.825	19	1.000
2	.841	20	1.000
3	.859	21	1.000
4	.879	22	1.000
5	.901	23	1.000
6	.922	24	1.000
7	.943	25	1.000
8	.962	26	.997
9	.978	27	.990
10	.990	28	.978
11	.997	29	.962
12	1.000	30	.943
13	1.000	31	.922
14	1.000	32	.901
15	1.000	33	.879
16	1.000	34	.859
17	1.000	35	.841
18	1.000	36	.825
Normalized vertical distance, x/H		Velocity ratio $s(x)$	
0.000		0.812	
.076		.838	
.129		.861	
.182		.886	
.235		.913	
.288		.940	
.341		.964	
.394		.983	
.447		.996	
.500		1.000	
.553		.996	
.606		.983	
.659		.964	
.712		.940	
.765		.913	
.818		.886	
.871		.861	
.924		.838	
1.000		.812	

TABLE 24.- 80x120 DESIGN LOAD
PARAMETERS--VANE SET 7

Parameters	Local lift Local drag	Global lift Global drag
c	10.54	10.54
H	---	197.2
h	17.8	---
Z	128.7	128.7
N	12	12
η_d	1.03	1.03
β_1	0	0
β_2	40	40
θ_1	0	0
$V_{0\max}$	62.8	62.8
ρ	.002385	.002385
Ω_b	1.5	1.5
TI_w	.149	.149
TI_u	.104	.104
s(x)	Flat profile	Flat profile
r_n	Flat profile	Flat profile
A_R	1.35	1.35

TABLE 25.- 40x80 LOAD ESTIMATES

Vane set	Lift (L) or drag (D)	Local (L) or global (G)	rms load, lb	Peak load, lb
1	L	L (11.4 ft)	636	1,590
	D	L (11.4 ft)	354	885
	D	L (68.6 ft)	1,345	3,364
	L	G	36,070	90,175
	D	G	27,030	67,575
2	L	L (11.4 ft)	450	1,125
	D	L (11.4 ft)	215	538
	D	L (68.6)	840	2,100
	L	G	36,000	90,000
	D	G	23,500	58,750
3	L	L (34 ft)	5,835	14,590
	D	L (34 ft)	218	545
	L	L (68.3 ft)	9,800	24,500
	D	L (68.3 ft)	387	968
5	L	L (25.1 ft)	457	1,143
	D	L (75.4 ft)	523	1,306
	L	G	16,040	40,100
	D	G	8,450	21,100
6	L	L (11 ft)	47	118
	D	L (11 ft)	29	74
	D	L (132.5 ft)	196	489
	L	G	2,530	6,325
	D	G	2,154	5,385
8	L	L (11 ft)	21	53
	D	L (11 ft)	13	33
	D	L (132.5 ft)	58	145
	L	G	3,354	8,385
	D	G	2,833	7,084

TABLE 26.- 80x120 LOAD ESTIMATES

Vane set	Lift (L) or drag (D)	Local (L) or global (G)	rms load, lb	Peak load, lb
4	L	L (34 ft)	431	1,080
	L	L (69.3 ft)	732	1,830
4 w/jet	L	L (34 ft)	5,054	12,640
	D	L (34 ft)	252	630
	L	L (69.3 ft)	8,693	21,740
	D	L (69.3 ft)	464	1,160
5	L	L (25.1 ft)	57	141
	L	L (75.4 ft)	115	287
	D	L (75.4 ft)	40	100
	L	G	658	1,645
	D	G	422	1,055
5 w/jet	L	L (25.1 ft)	631	1,578
	D	L (25.1 ft)	226	565
	L	L (75.4 ft)	1,372	3,430
	D	L (75.4 ft)	480	1,200
	L	G	15,050	37,600
	D	G	7,110	17,800
7	L	L (17.8 ft)	112	280
	D	L (17.8 ft)	107	268
	L	G	1,332	3,330
	D	G	853	2,133

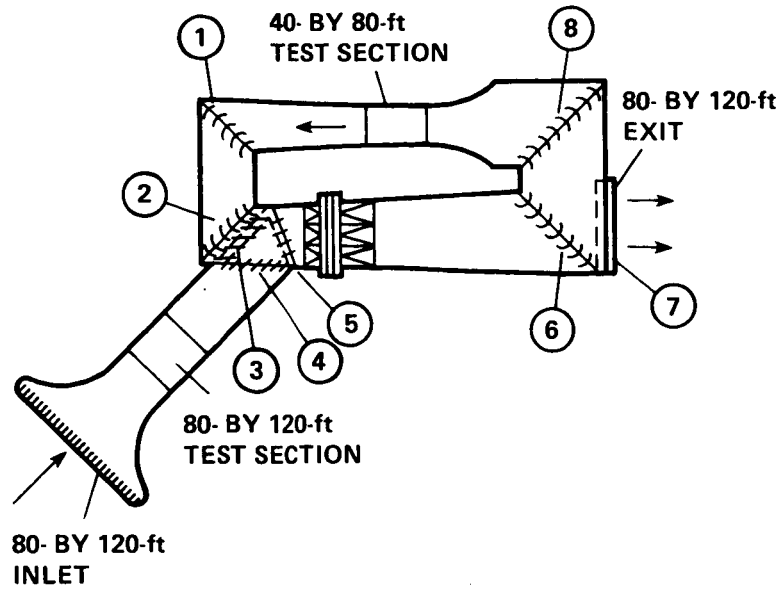


Figure 1.- Plan view of NFAC showing vane set locations.

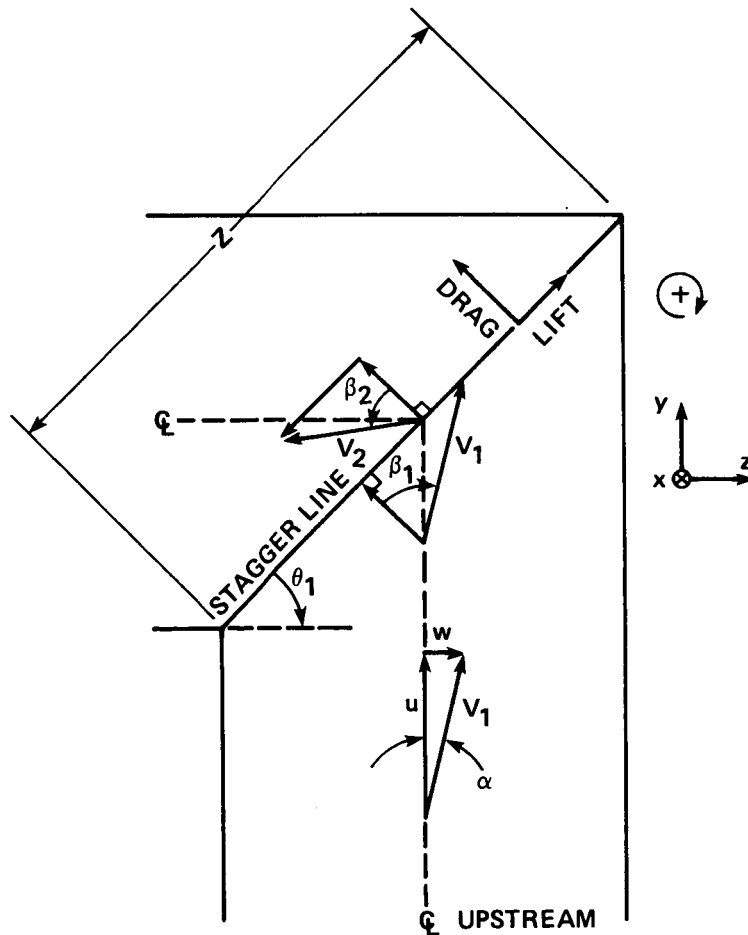


Figure 2.- Definitions and sign conventions for analysis.

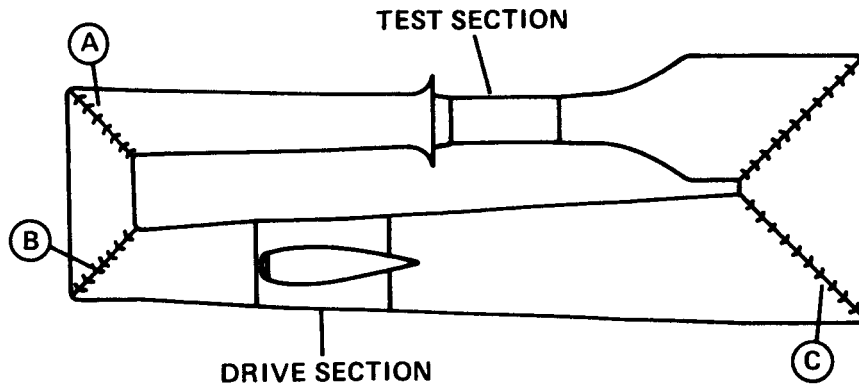


Figure 3.- NASA Langley 4 x 7 m wind tunnel showing vane set locations.

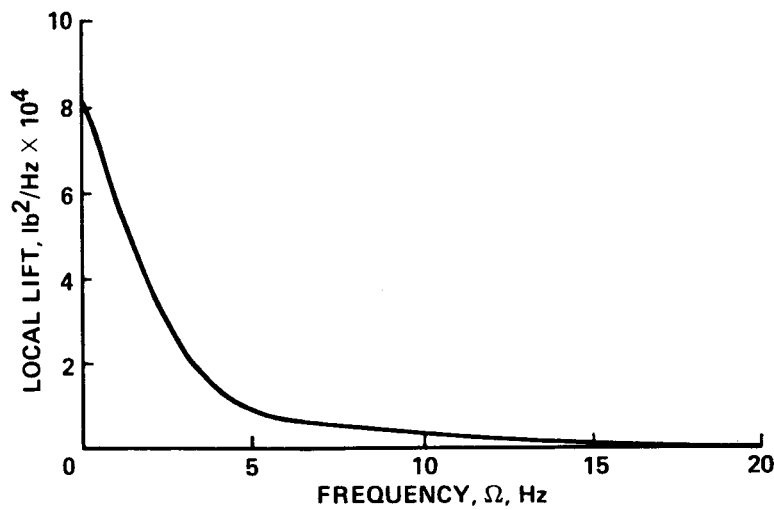


Figure 4.- Local lift spectrum for 11.4-ft section of vane set 1.
 $\sigma = 636 \text{ lb}$, peak load = 1590 lb.

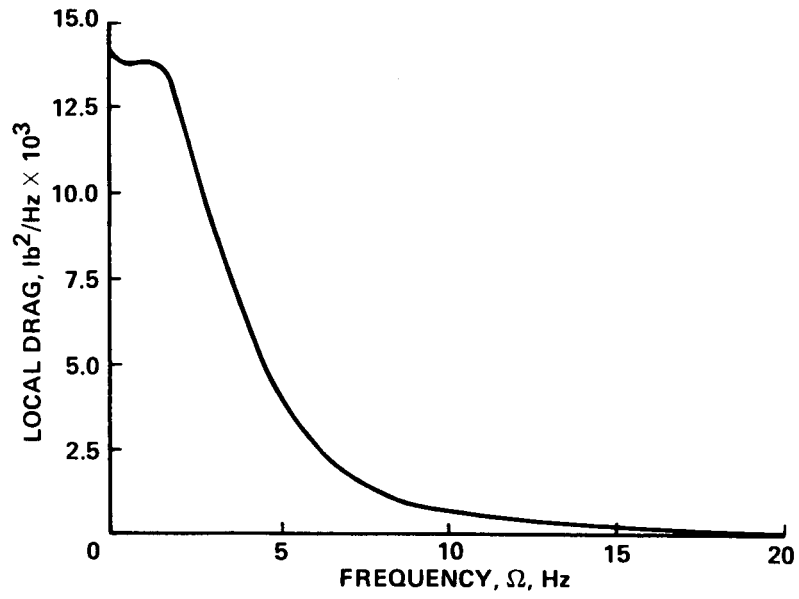


Figure 5.- Local drag spectrum for 11.4-ft section of vane set 1.
 $\sigma = 354$ lb, peak load = 885 lb.

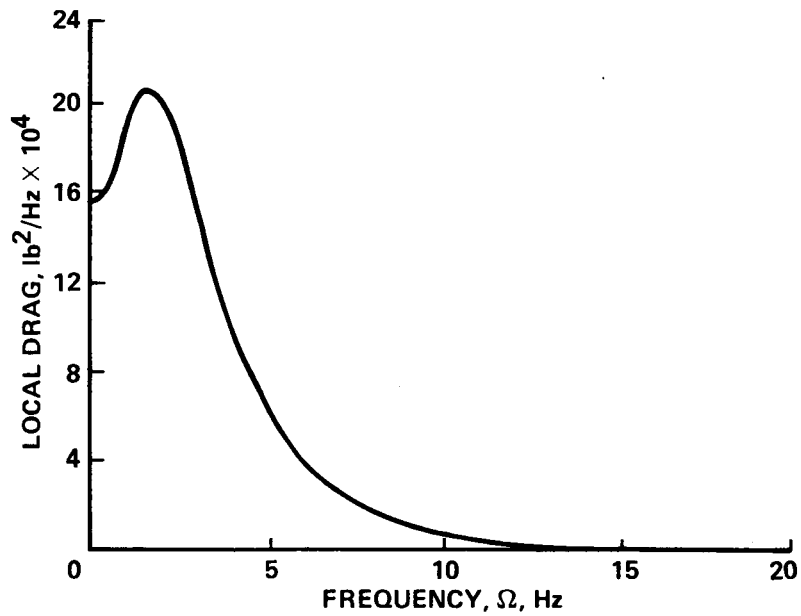


Figure 6.- Local drag spectrum for 68.6 ft section of vane set 1.
 $\sigma = 1345$ lb, peak load = 3364 lb.

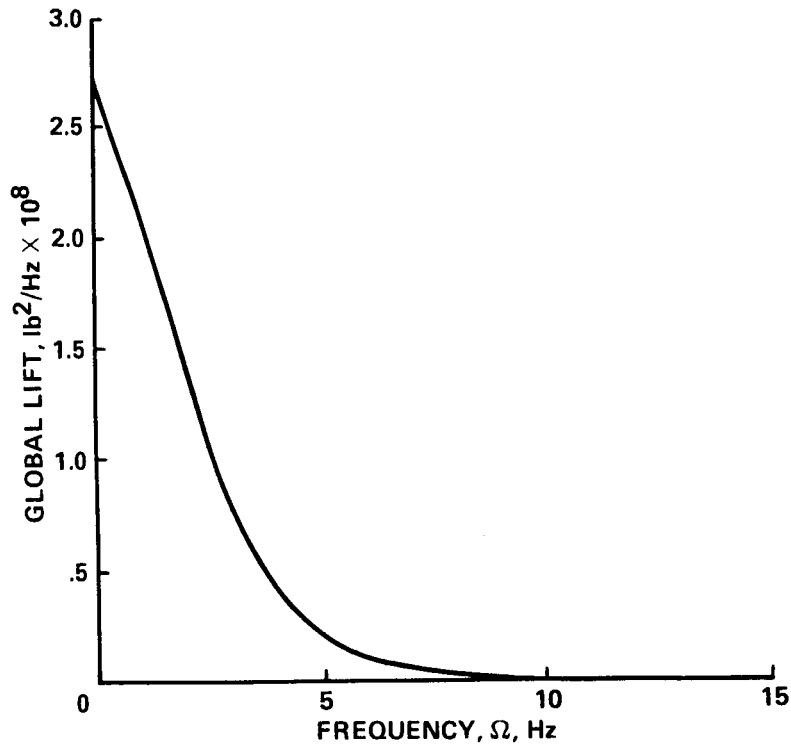


Figure 7.- Global lift spectrum for vane set 1.
 $\sigma = 36,070$ lb, peak load = 90,175 lb.

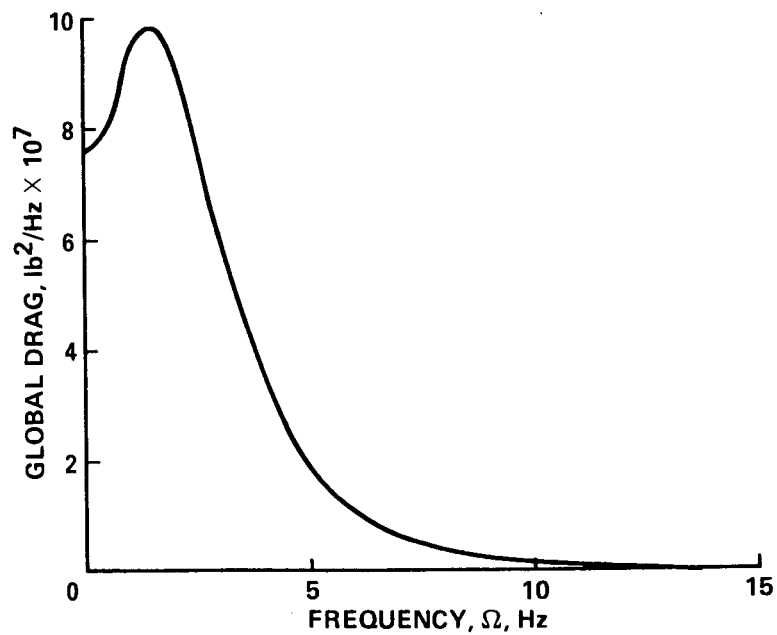


Figure 8.- Global drag spectrum for vane set 1.
 $\sigma = 27,030$ lb, peak load = 67,575 lb.

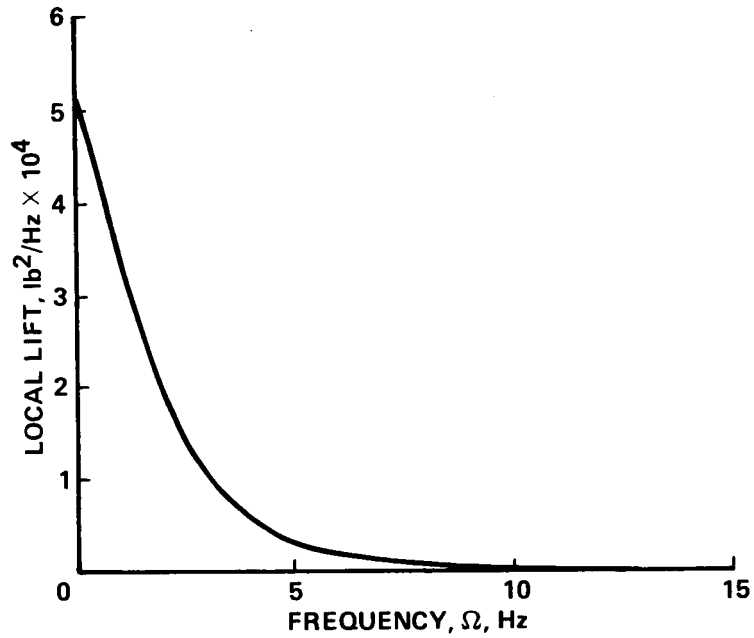


Figure 9.- Local lift spectrum for 11.4-ft section of vane set 2.
 $\sigma = 450$ lb, peak load = 1125 lb.

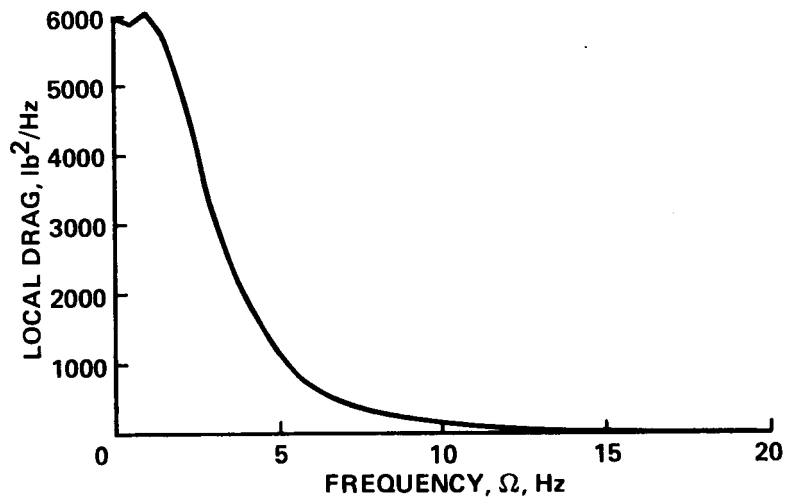


Figure 10.- Local drag spectrum for 11.4-ft section of vane set 2.
 $\sigma = 215$ lb, peak load = 538 lb.

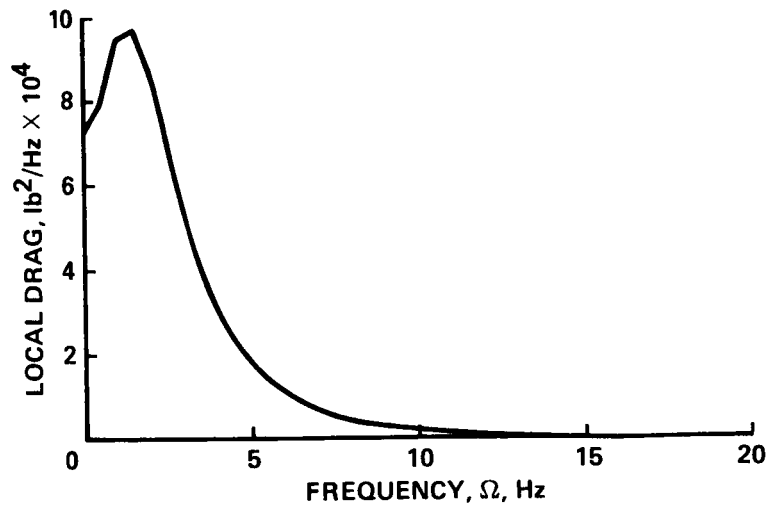


Figure 11.- Local drag spectrum for 68.6-ft section of vane set 2.
 $\sigma = 840 \text{ lb}$, peak load = 2100 lb.

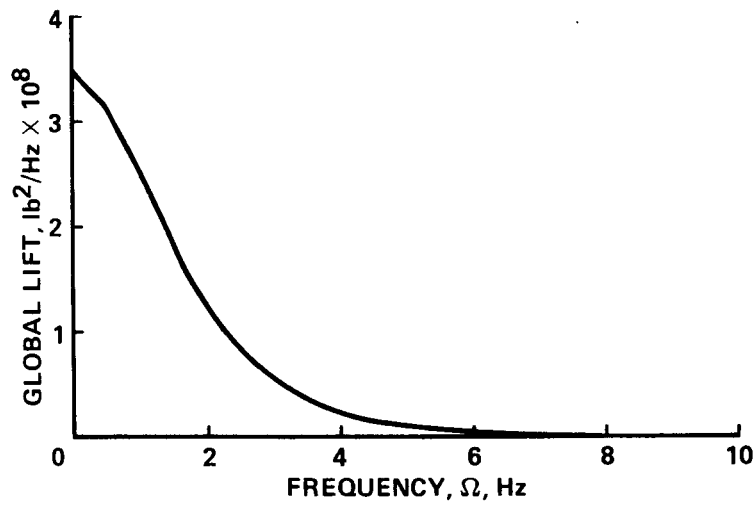


Figure 12.- Global lift spectrum for vane set 2.
 $\sigma = 36,000 \text{ lb}$, peak load = 90,000 lb.

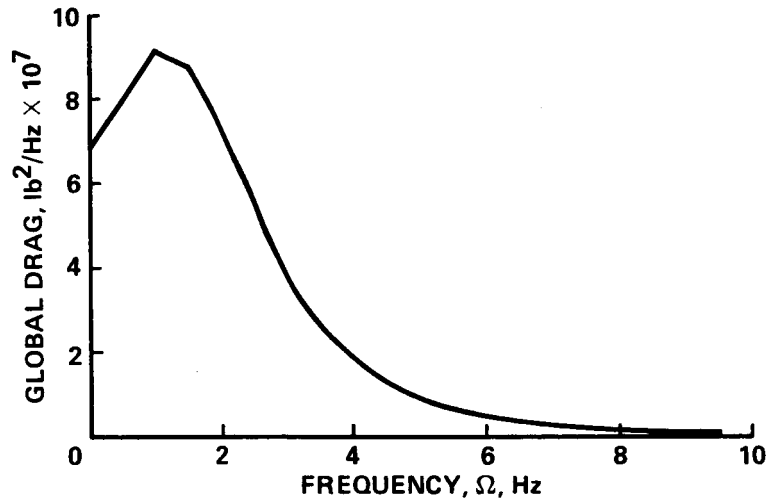


Figure 13.- Global drag spectrum for vane set 2.
 $\sigma = 23,500$ lb, peak load = 58,750 lb.

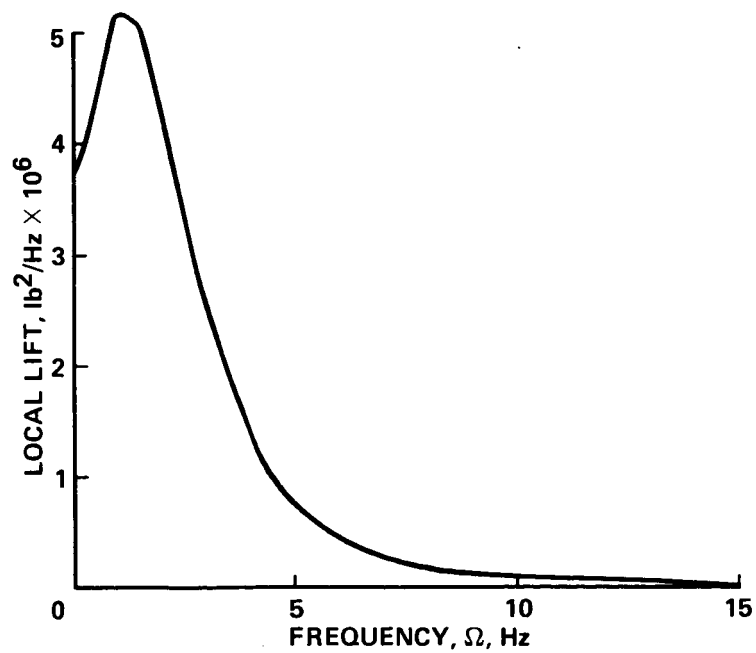


Figure 14.- Local lift spectrum for 34-ft section of vane set 3.
 $\sigma = 5835$ lb, peak load = 14,590 lb.

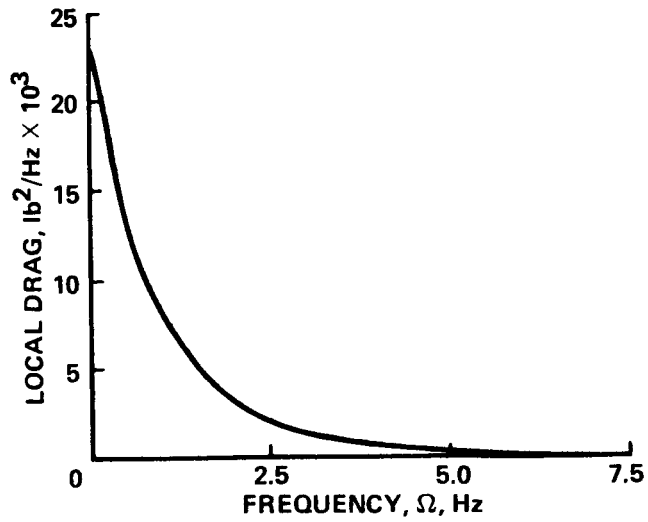


Figure 15.- Local drag spectrum for 34-ft section of vane set 3.
 $\sigma = 218 \text{ lb}$, peak load = 545 lb.

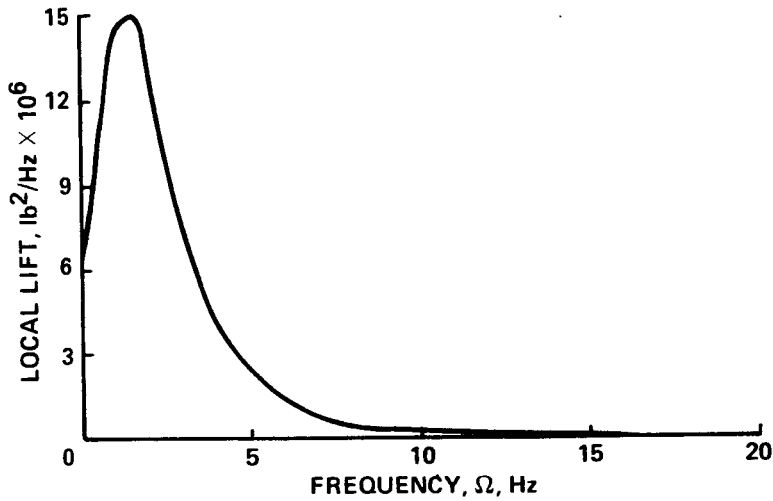


Figure 16.- Local lift spectrum for 68.3-ft section of vane set 3.
 $\sigma = 9800 \text{ lb}$, peak load = 24,500 lb.

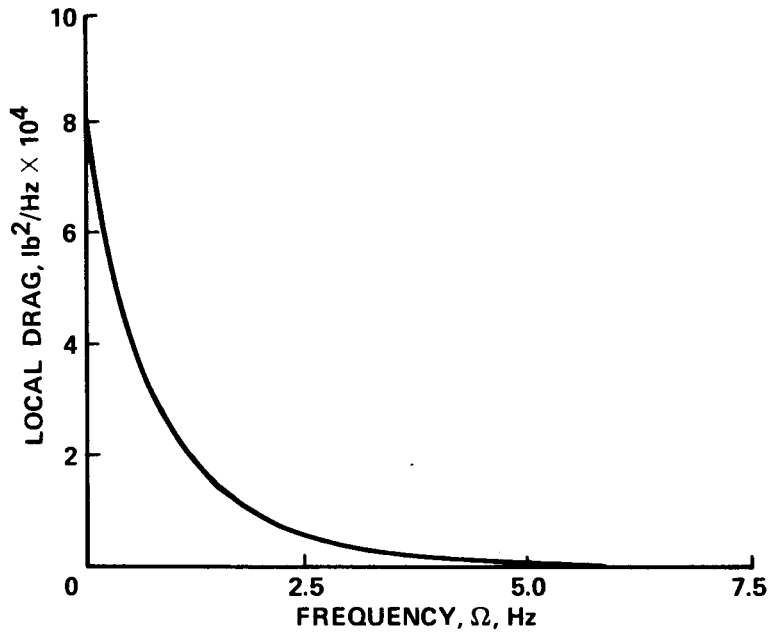


Figure 17.- Local drag spectrum for 68.3-ft section of vane set 3.
 $\sigma = 387$ lb, peak load = 968 lb.

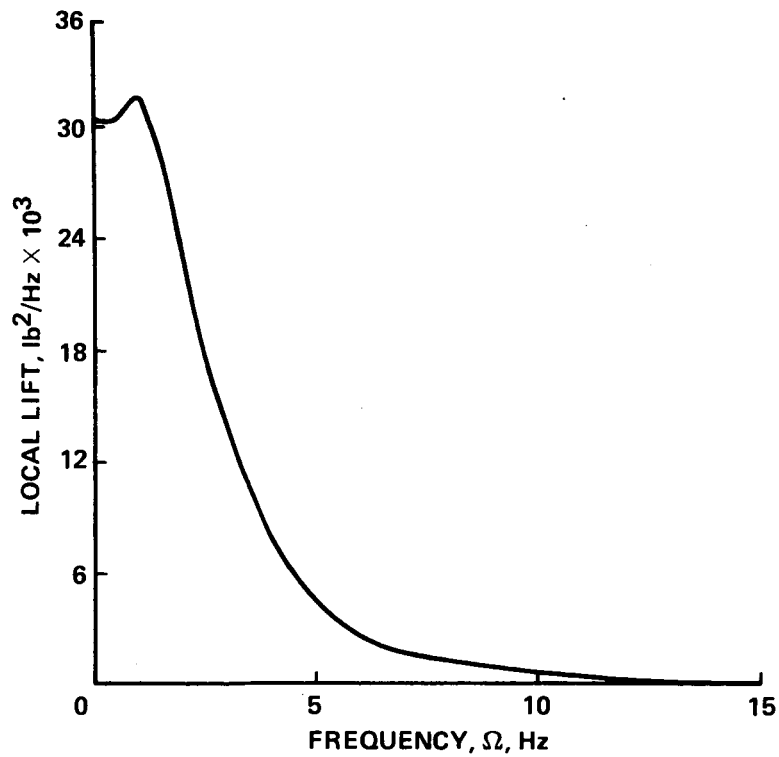


Figure 18.- Local lift spectrum for 25.1-ft section of vane set 5, 40x80.
 $\sigma = 457$ lb, peak load = 1143 lb.

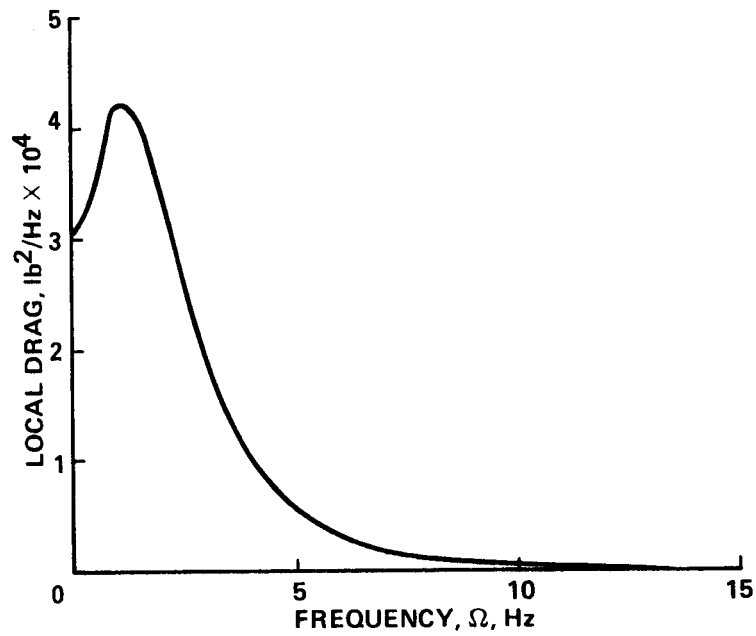


Figure 19.- Local drag spectrum for 75.4-ft section of vane set 5, 40x80.
 $\sigma = 523$ lb, peak load = 1306 lb.

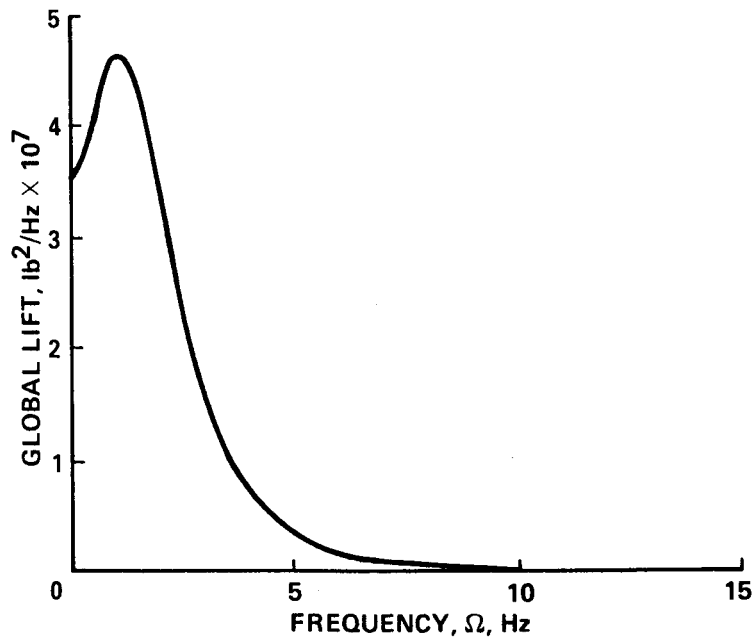


Figure 20.- Global lift spectrum for vane set 5, 40x80.
 $\sigma = 16,040$ lb, peak load = 40,100 lb.

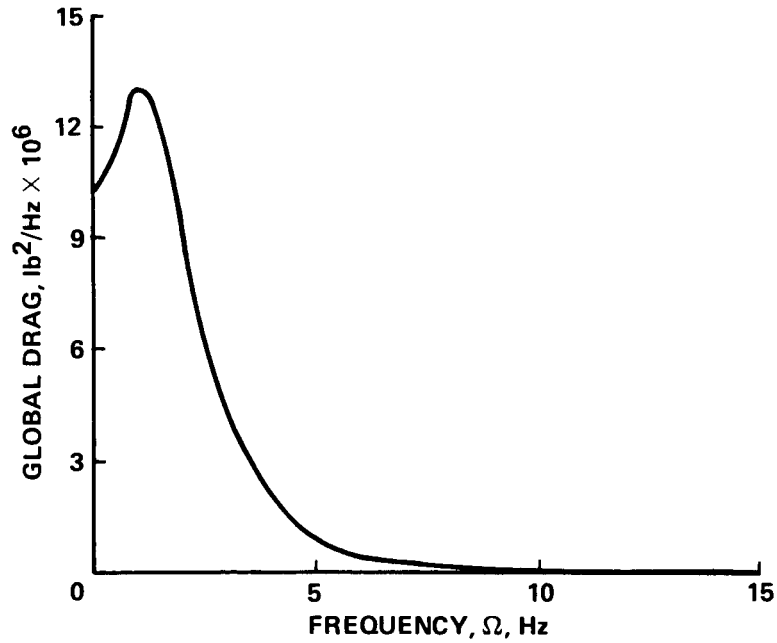


Figure 21.- Global drag spectrum for vane set 5, 40x80.
 $\sigma = 8450 \text{ lb}$, peak load = 21,100 lb.

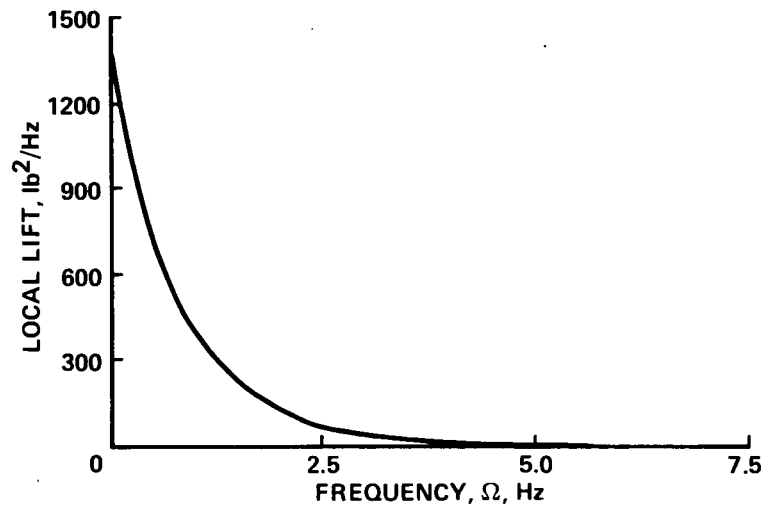


Figure 22.- Local lift spectrum for 11-ft section of vane set 6.
 $\sigma = 47 \text{ lb}$, peak load = 118 lb.

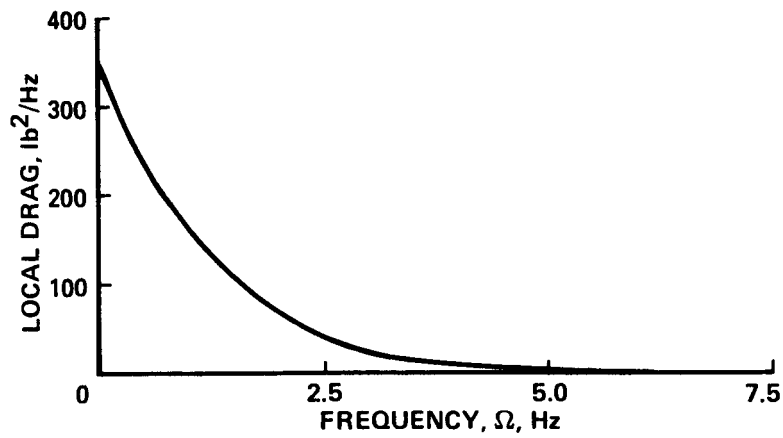


Figure 23.- Local drag spectrum for 11-ft section of vane set 6.
 $\sigma = 29$ lb, peak load = 74 lb.

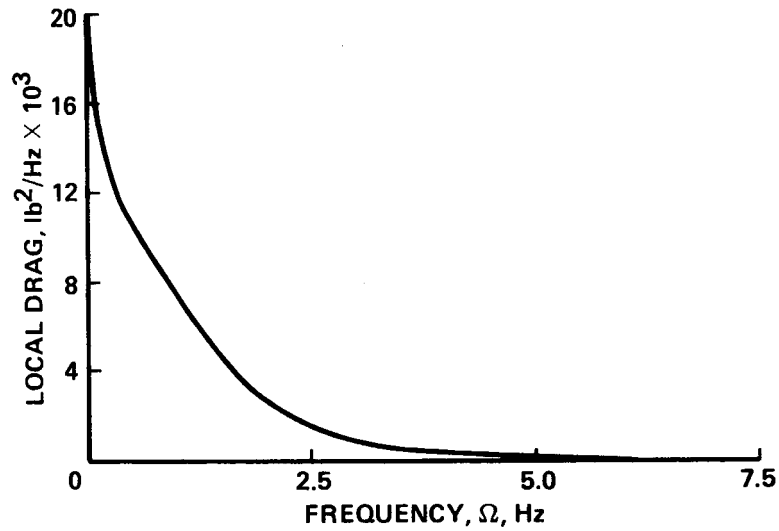


Figure 24.- Local drag spectrum for 132.5-ft section of vane set 6.
 $\sigma = 196$ lb, peak load = 489 lb.

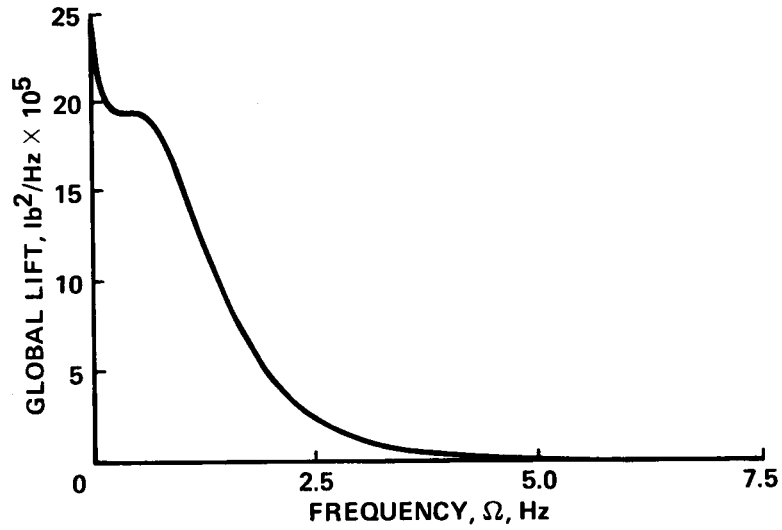


Figure 25.- Global lift spectrum for vane set 6.
 $\sigma = 2530$ lb, peak load = 6325 lb.

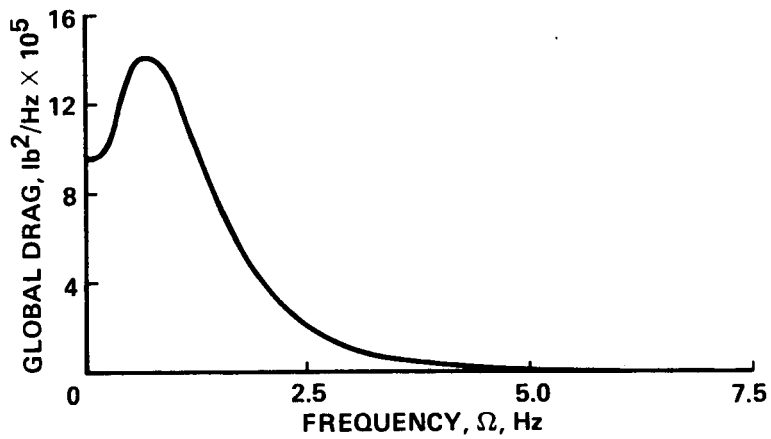


Figure 26.- Global drag spectrum for vane set 6.
 $\sigma = 2154$ lb, peak load = 5385 lb.

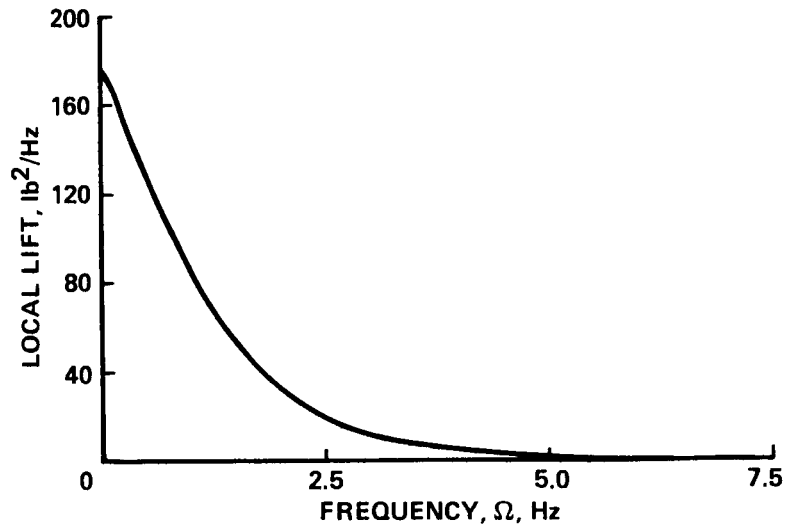


Figure 27.- Local lift spectrum for 11-ft section of vane set 8.
 $\sigma = 21$ lb, peak load = 53 lb.

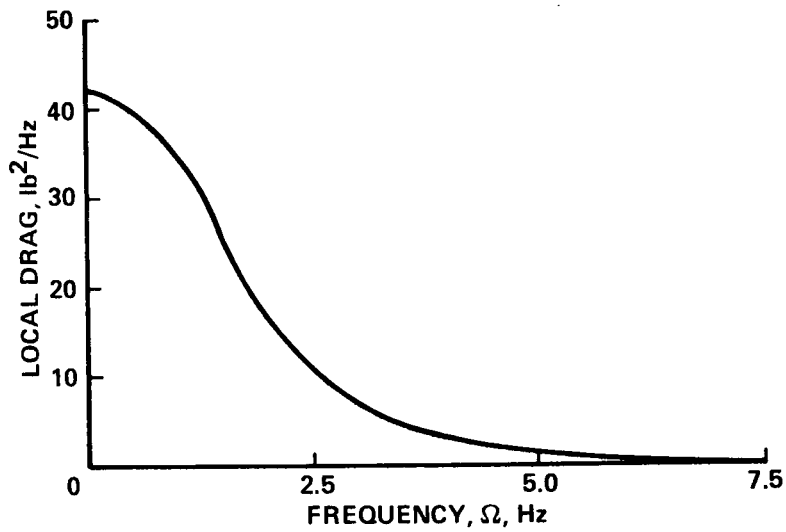


Figure 28.- Local drag spectrum for 11-ft section of vane set 8.
 $\sigma = 13$ lb, peak load = 33 lb.

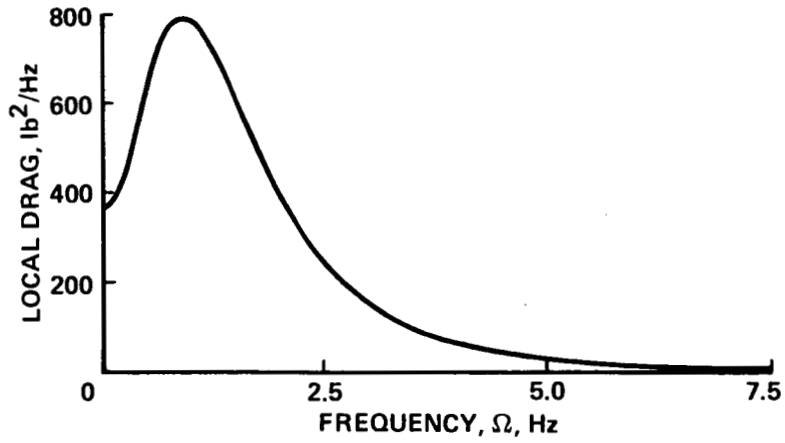


Figure 29.- Local drag spectrum for 132.5-ft section of vane set 8.
 $\sigma = 58 \text{ lb}$, peak load = 145 lb.

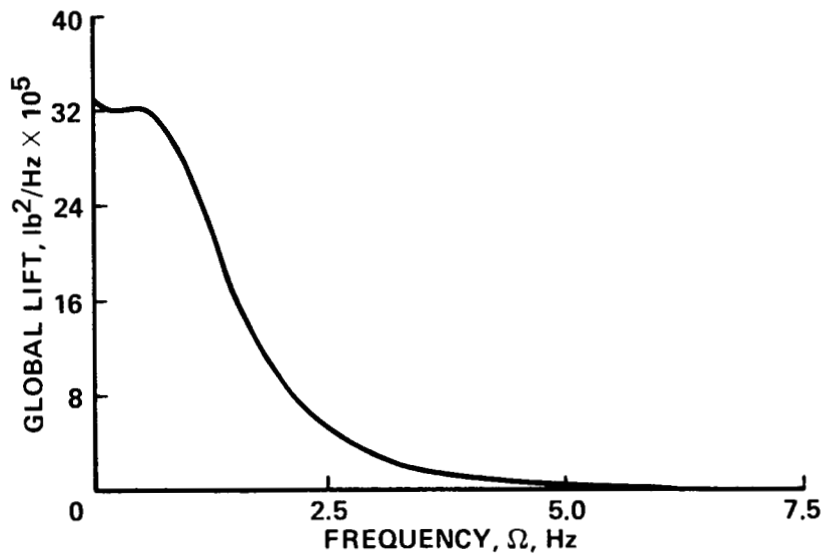


Figure 30.- Global lift spectrum for vane set 8.
 $\sigma = 3354 \text{ lb}$, peak load = 8385 lb.

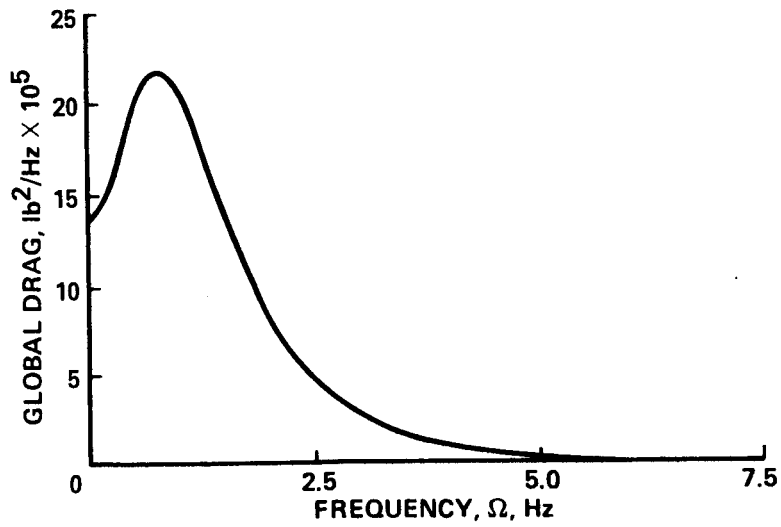


Figure 31.- Global drag spectrum for vane set 8.
 $\sigma = 2833$ lb, peak load = 7084 lb.

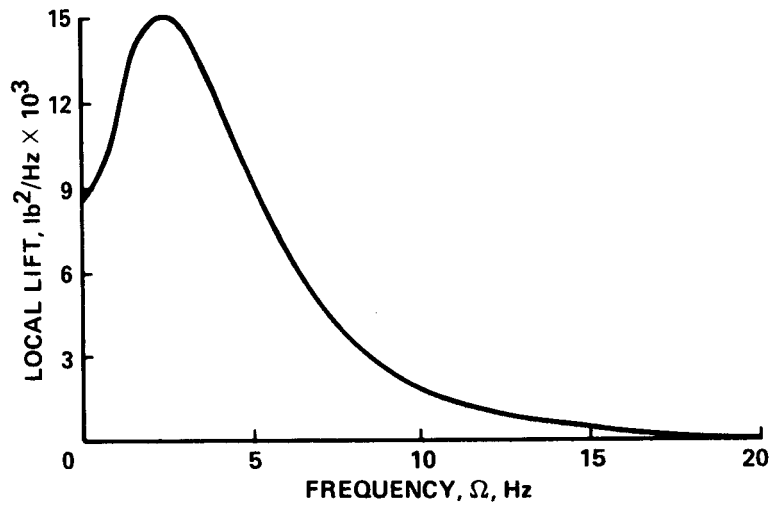


Figure 32.- Local lift spectrum for 34-ft section of vane set 4.
 $\sigma = 431$ lb, peak load = 1080 lb.

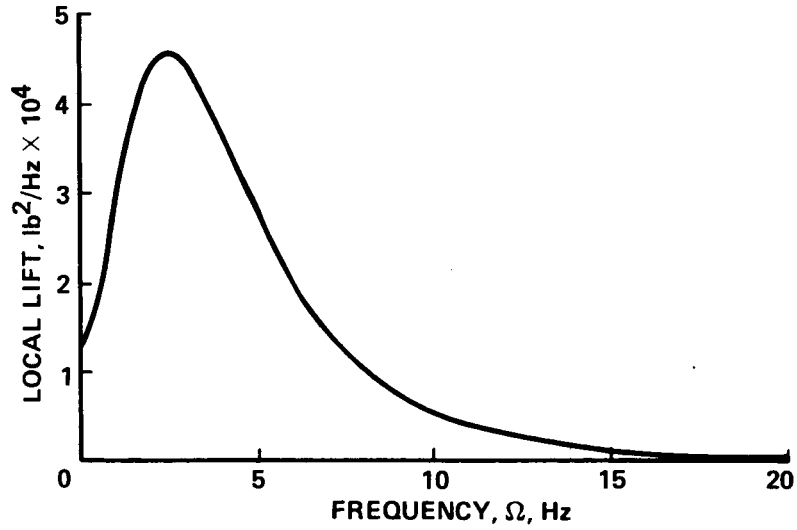


Figure 33.- Local lift spectrum for 69.3-ft section of vane set 4.
 $\sigma = 732$ lb, peak load = 1830 lb.

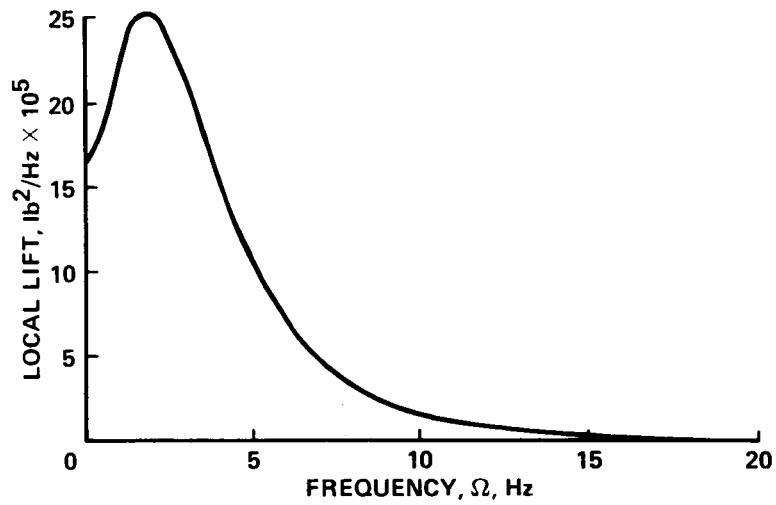


Figure 34.- Local lift spectrum for 34-ft section of vane set 4, with test section jet. $\sigma = 5054$ lb, peak load = 12,640 lb.

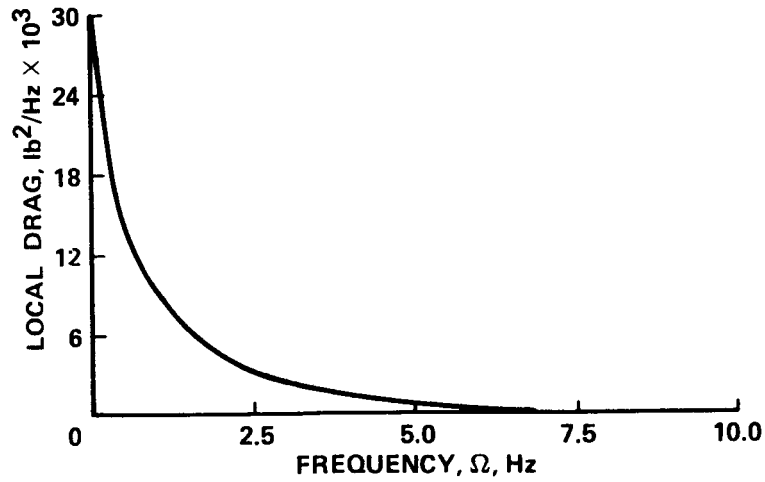


Figure 35.- Local drag spectrum for 34-ft section of vane set 4, with test section jet. $\sigma = 252$ lb, peak load = 630 lb.

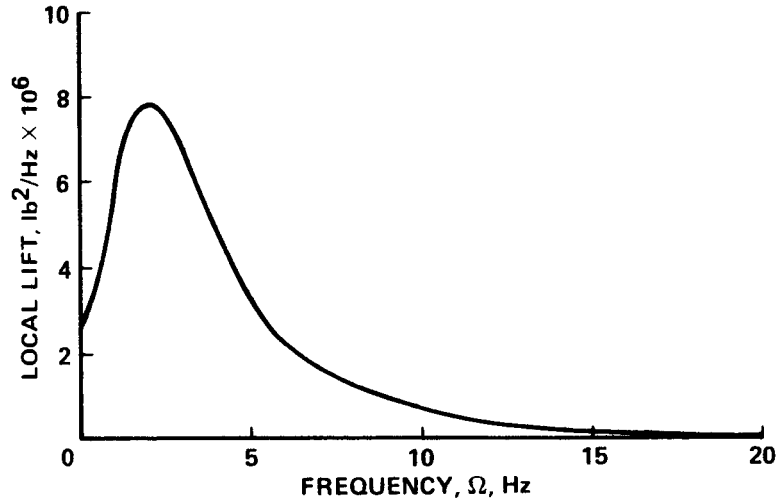


Figure 36.- Local lift spectrum for 69.3-ft section of vane set 4, with test section jet. $\sigma = 8693$ lb, peak load = 21,740 lb.

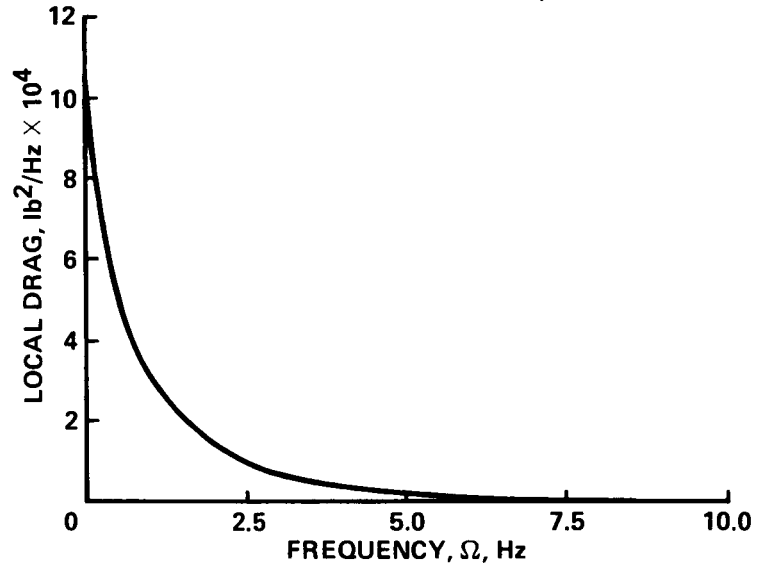


Figure 37.- Local drag spectrum for 69.3-ft section of vane set 4, with test section jet. $\sigma = 464$ lb, peak load = 1160 lb.

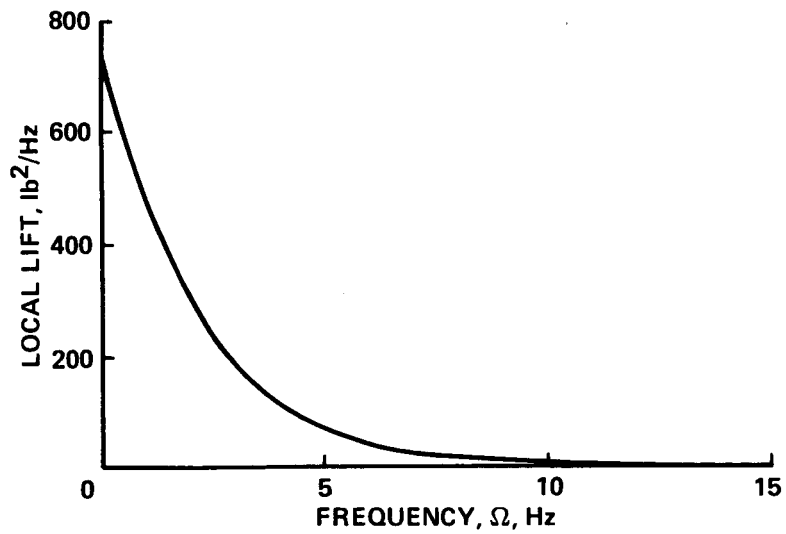


Figure 38.- Local lift spectrum for 25.1-ft section of vane set 5, 80x120. $\sigma = 57$ lb, peak load = 141 lb.

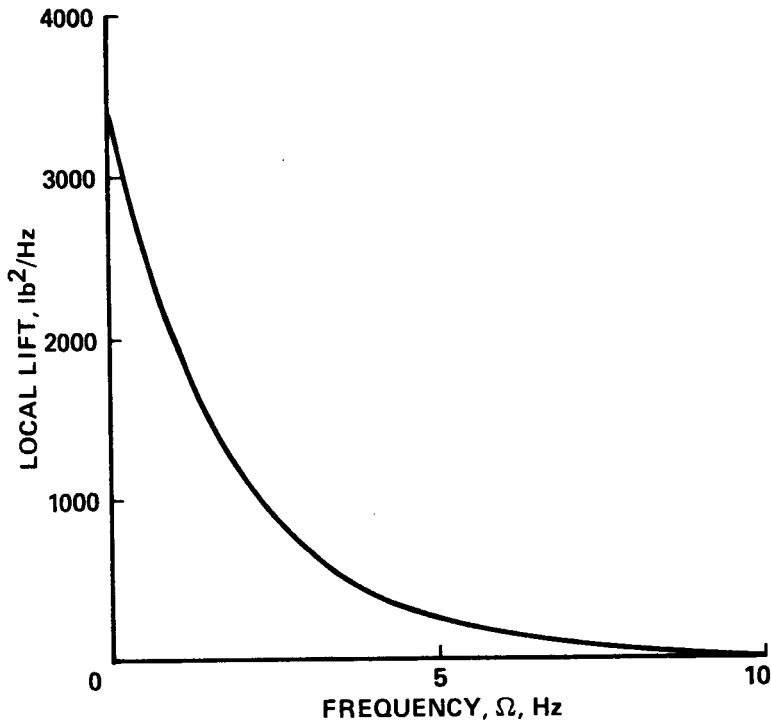


Figure 39.- Local lift spectrum for 75.4-ft section of vane set 5, 80x120.
 $\sigma = 115 \text{ lb}$, peak load = 287 lb.

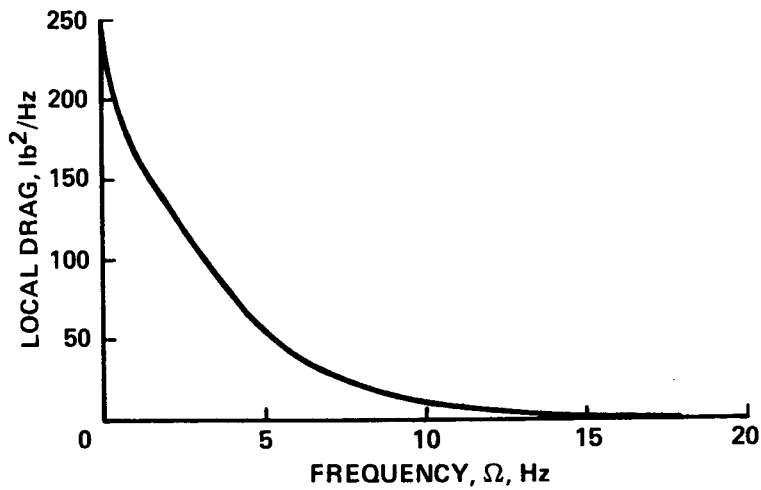


Figure 40.- Local drag spectrum for 75.4-ft section of vane set 5, 80x120.
 $\sigma = 40 \text{ lb}$, peak load = 100 lb.

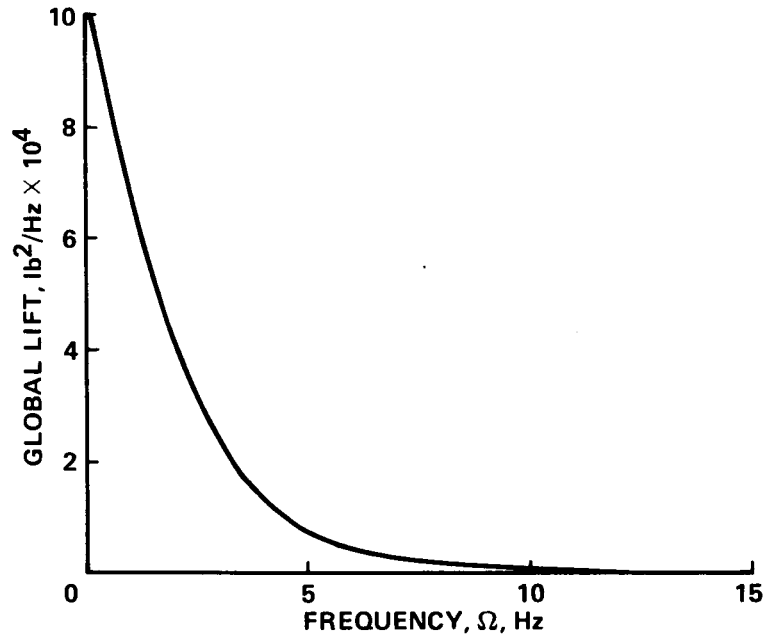


Figure 41.- Global lift spectrum for vane set 5, 80x120.
 $\sigma = 658$ lb, peak load = 1645 lb.

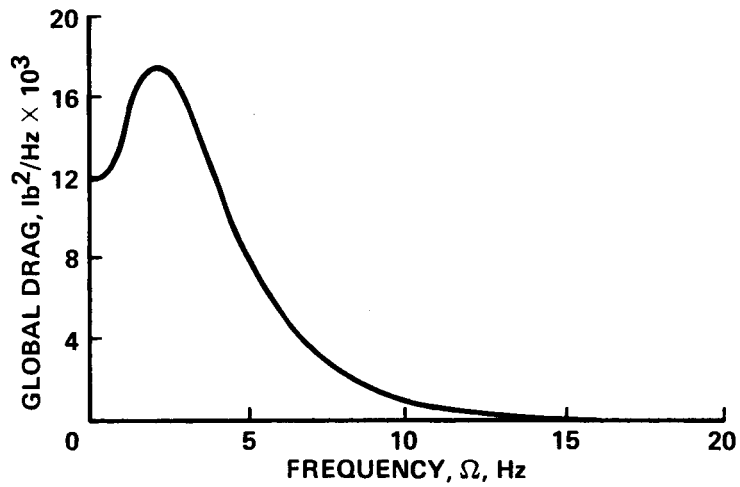


Figure 42.- Global drag spectrum for vane set 5, 80x120.
 $\sigma = 422$ lb, peak load = 1055 lb.

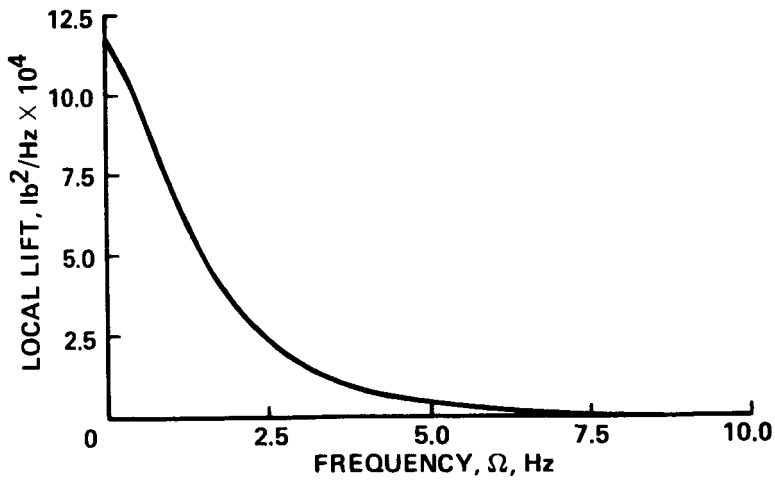


Figure 43.- Local lift spectrum for 25.1-ft section of vane set 5, 80x120, with test section jet. $\sigma = 631$ lb, peak load = 1578 lb.

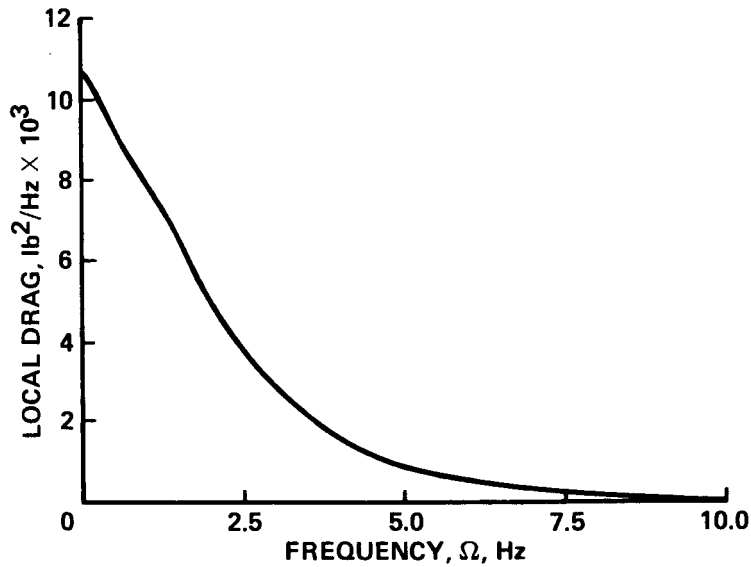


Figure 44.- Local drag spectrum for 25.1-ft section of vane set 5, 80x120, with test section jet. $\sigma = 226$ lb, peak load = 565 lb.

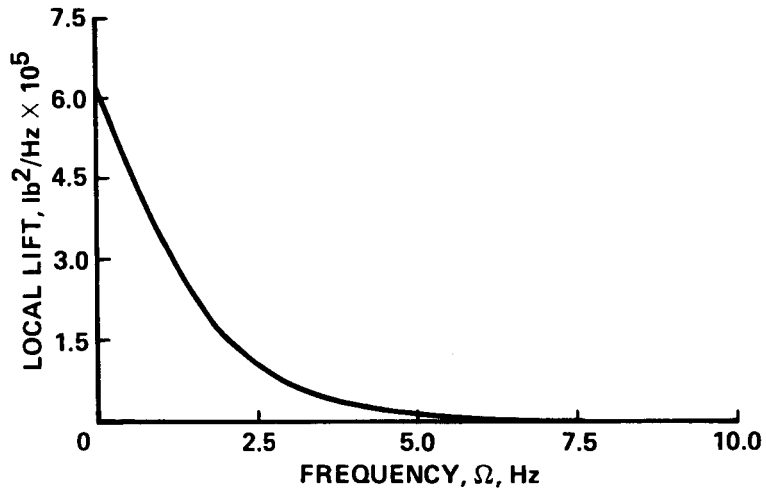


Figure 45.- Local lift spectrum for 75.4-ft section of vane set 5, 80x120, with test section jet. $\sigma = 1372$ lb, peak load = 3430 lb.

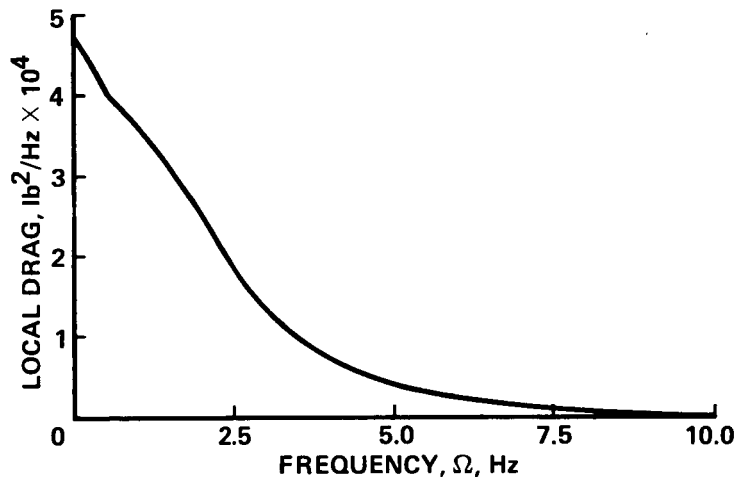


Figure 46.- Local drag spectrum for 75.4-ft section of vane set 5, 80x120, with test section jet. $\sigma = 480$ lb, peak load = 1200 lb.

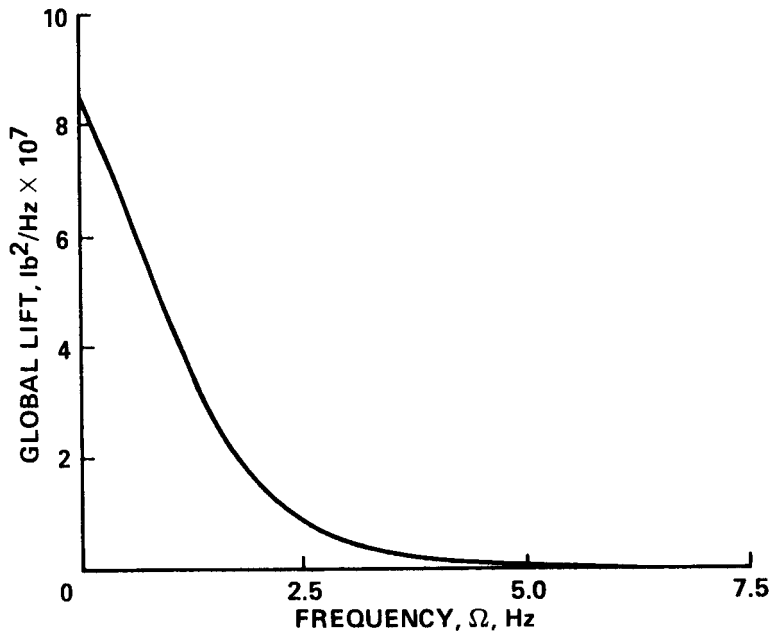


Figure 47.- Global lift spectrum for vane set 5, 80x120, with test section jet.
 $\sigma = 15,050$ lb, peak load = 37,600 lb.

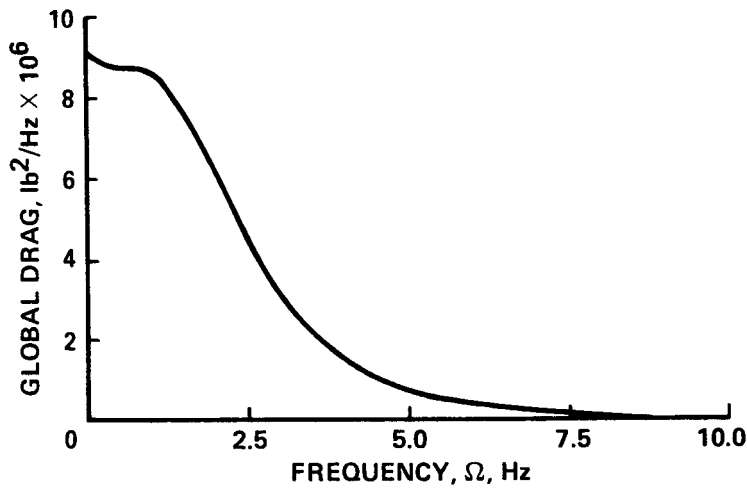


Figure 48.- Global drag spectrum for vane set 5, 80x120, with test section jet.
 $\sigma = 7110$ lb, peak load = 17,800 lb.

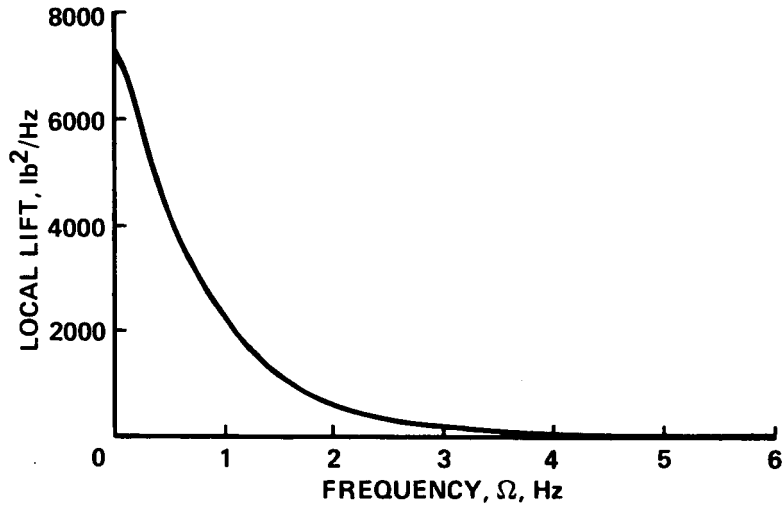


Figure 49.- Local lift spectrum for 17.8-ft section of vane set 7.
 $\sigma = 112 \text{ lb}$, peak load = 280 lb.

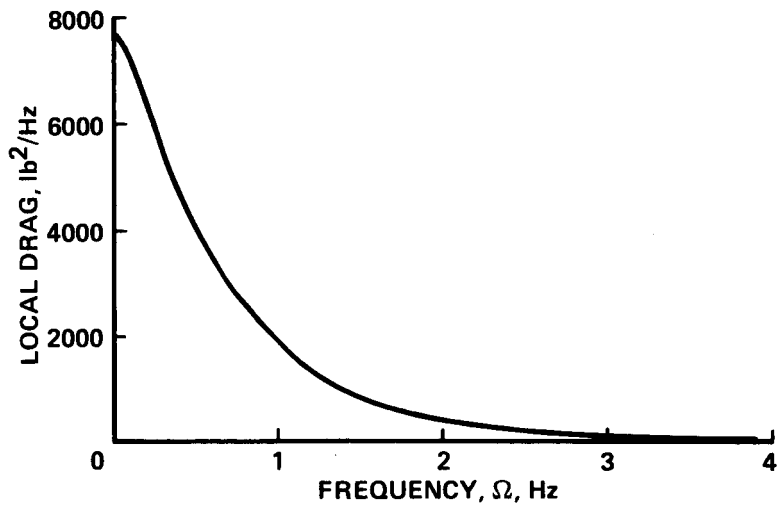


Figure 50.- Local drag spectrum for 17.8-ft section of vane set 7.
 $\sigma = 107 \text{ lb}$, peak load = 268 lb.

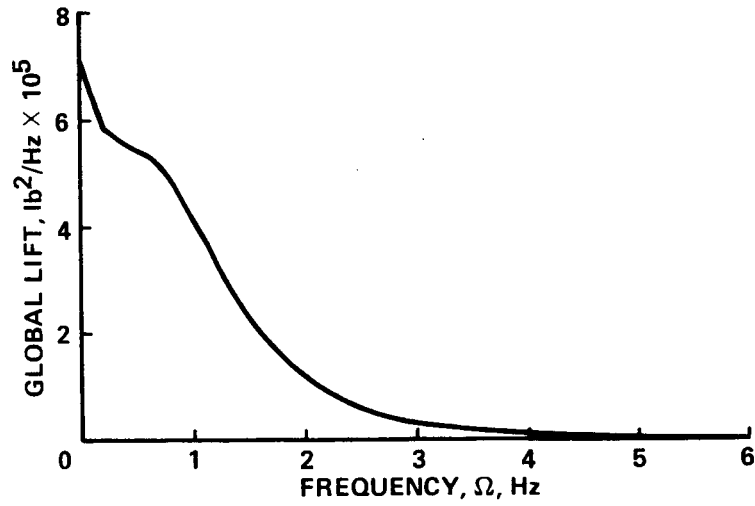


Figure 51.- Global lift spectrum for vane set 7.
 $\sigma = 1332$ lb, peak load = 3330 lb.

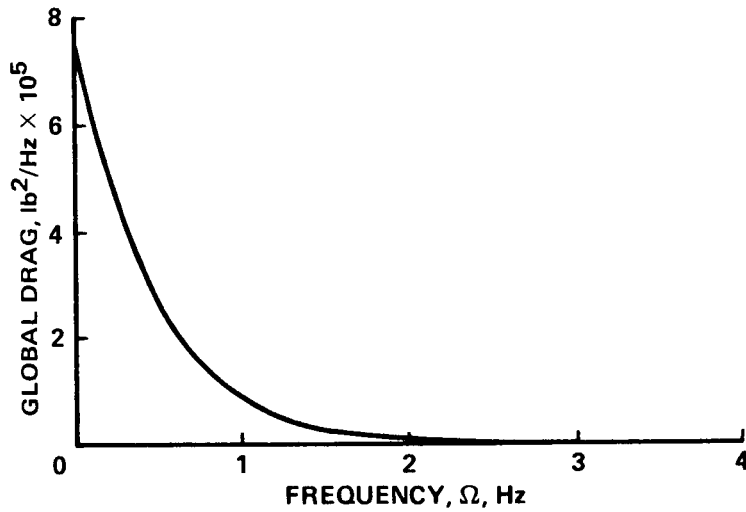


Figure 52.- Global drag spectrum for vane set 7.
 $\sigma = 853$ lb, peak load = 2133 lb.

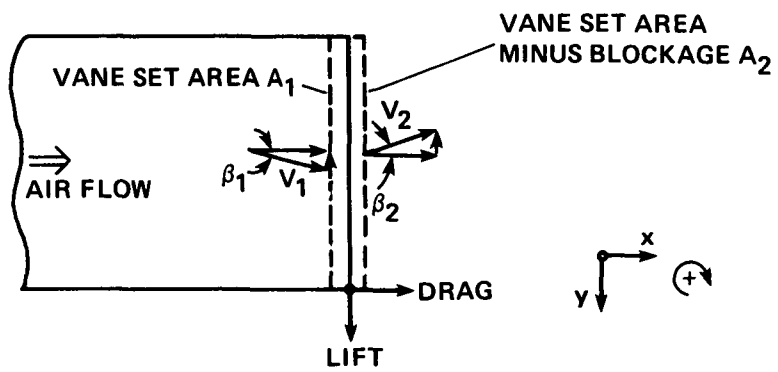


Figure 53.- Definitions and sign conventions for vane set 7 variables.

1. Report No. NASA TM-88191		2. Government Accession No.		3. Recipient's Catalog No.	
4. Title and Subtitle UNSTEADY AERODYNAMIC LOAD ESTIMATES ON TURNING VANES IN THE NATIONAL FULL-SCALE AERODYNAMIC COMPLEX				5. Report Date December 1986	
				6. Performing Organization Code	
7. Author(s) Thomas R. Norman				8. Performing Organization Report No. A-86015	
9. Performing Organization Name and Address Ames Research Center Moffett Field, CA 94035				10. Work Unit No.	
				11. Contract or Grant No.	
12. Sponsoring Agency Name and Address National Aeronautics and Space Administration Washington, DC 20546				13. Type of Report and Period Covered Technical Memorandum	
				14. Sponsoring Agency Code 505-42-11	
15. Supplementary Notes Point of Contact: Thomas R. Norman, Ames Research Center, MS 247-1, Moffett Field, CA 94035, (415)694-6653 or FTS 464-6653					
16. Abstract <p>Unsteady aerodynamic design loads have been estimated for each of the vane sets in the National Full-Scale Aerodynamic Complex (NFAC). These loads include estimates of local loads over one vane section and global loads over an entire vane set. The analytical methods and computer programs used to estimate these loads are discussed in this paper. In addition, the important computer input parameters are defined and the rationale used to estimate them is discussed. Finally, numerical values are presented for both the computer input parameters and the calculated design loads for each vane set.</p>					
17. Key Words (Suggested by Author(s)) Wind tunnels Unsteady aerodynamics Cascade aerodynamics Vane sets				18. Distribution Statement Unclassified - Unlimited Subject category - 02	
19. Security Classif. (of this report) Unclassified		20. Security Classif. (of this page) Unclassified		21. No. of Pages 75	22. Price* A05